Applied Thermal Engineering 299 (2026) 131038

Contents lists available at ScienceDirect

Applied Thermal Engineering

journal homepage: www.elsevier.com/locate/ate

Research Paper

Assessing the economic viability of thermography-based leak detection for district heating systems

Elena Vollmer [a,*], Rebekka Volk [b], Frank Schultmann [a]

[a] Karlsruhe Institute of Technology (KIT), Institute for Industrial Production (IIP), Hertzstr. 16, Karlsruhe, 76187, Baden-Wuerttemberg, Germany
[b] University of Freiburg, Sustainability Assessment of Technical Systems (INATECH), Emmy-Noether-Str. 2, Freiburg, 79110, Baden-Wuerttemberg, Germany

ARTICLE INFO

Keywords:
Break-even analysis
District heating
Leak detection
Pipeline leak modelling
Remote sensing
Thermography

ABSTRACT

District heating systems (DHSs) play a central role in Europe's sustainable heat transition, yet pipeline leaks threaten their efficiency and reliability. Thermography-based leak detection (TLD), particularly via remote sensing, has emerged as a promising non-invasive localisation approach, however its cost-effectiveness remains unexplored.

This study presents the first quantitative economic assessment of TLD for DHS pipeline leak detection based on newly collected empirical data centred around Central European German-speaking countries. To this end, leak growth and associated ongoing and repair costs are modelled and a break-even analysis is performed to compare TLD to baseline operational scenarios. The results show that TLD can recover its costs within months after deployment, even under conservative assumptions, and consistently outperforms passive leak response strategies. Based on these findings, the study offers recommendations for integrating TLD into network monitoring strategies and contributes to the broader evaluation of innovative and cost-efficient leak detection methods for DHS operators.

1. Introduction

1.1. Context

In light of the ongoing energy crisis, securing sustainable and resilient heat supply systems has become a central concern for policymakers and urban planners in Europe. Among the most promising technologies in this regard are DHSs, which provide thermal energy to buildings through centralised heat production and distribution networks. These systems, of which there are more than 19,000 in the EU alone [1], have evolved to offer efficient, sustainable, and cost-effective alternatives to decentralised, fossil-fuel-based heating [2]. In Denmark, where two-thirds of the population receive 89 % climate-neutral heat via DHSs [3], such networks are already forming the backbone of a low-carbon heating strategy.

However, maintaining DHS efficiency and reliability is vital, especially as the components age and deteriorate over time. In Germany, network losses have consistently ranged between 10 % to 14 % over the past two decades [3]. A key contributor to these losses are leaks in the underground transport pipelines, the most failure-prone component of DHSs [4,5]. Left undetected, such leaks not only reduce efficiency but also risk escalating into severe infrastructural damage and high repair costs [6,7]. With around 600,000 km of pipelines in operation worldwide [5] – a third of which lie within the EU [1,8] – this issue presents a major challenge.

To address it, various LD approaches have been developed, including conventional tools like integrated leak detection systems (ILDSs) or novel techniques such as correlators, tracer gas, or thermography. TIR imaging, especially when remotely sensed, enables the non-invasive, flexible localisation of heat anomalies that may indicate underground pipeline leaks [6,9]. However, despite algorithmic and technological advances in this field, the critical question of economic viability remains unanswered.

1.2. Related work

Thermography is mentioned as a promising and robust option for LD in DHS pipelines in various reviews, notably Zhou et al. [10] and Latif et al. [11]. Several studies have explored TLD as a technical solution. Foundational research by Ljungberg and Rosengren [12] and Axelsson [13] demonstrated that underground leaks in DHSs lead to measurable hot-spots on the surface. More recent efforts have advanced the algorithmic analysis of TIR data, leveraging computer vision to improve detection accuracy and reduce false positives to present operators with a viable list of leak candidates. These range from histogram-based [6,9,

* Corresponding author.
E-mail address: elena.vollmer@kit.edu (E. Vollmer).

https://doi.org/10.1016/j.applthermaleng.2026.131038
Received 5 January 2026; Received in revised form 26 March 2026; Accepted 13 April 2026
Available online 20 April 2026

14,15], over saliency mapping [9,16,17], to machine and deep learning methods [14,18,19].

However, the economic dimension of this particular approach has received little attention. Existing work typically focusses on technical feasibility or data processing methods, with no assessment of operational costs or financial BEPs. This may be attributed to the novelty of TLD, from which follows a lack of data with which to quantify the economy of all process steps and involved aspects — not just regarding the method itself, but also the economic impact of leaks on DHSs. So far, only Tuikka [20] provide an overview of LD methods used by Finnish DHS operators from a practical perspective to shed light on cost-effectiveness and reliability. However, they so do in a strictly qualitative manner and without a specific focus on TLD. Some newer reviews such as Ye et al. [21] provide indicative comparisons of LD technologies and occasionally report approximate costs for select approaches, but these are context-specific and do not constitute a systematic economic evaluation of LD strategies.

Indeed, a recent review by Ahmed et al. [22] highlights this lack of monetising economic benefits as a general problem in DHS research. While a growing number of publications showcase ways of improving DHS design, operation, and management, only around 10 % quantify approaches in monetary terms and even fewer detail their methodology [22]. In general, existing studies revolve around the impact of alternate energy sources [23,24] or operating conditions [25]. This finding is mirrored by Ahmed et al. [22]'s comprehensive overview, which is not able to identify any studies pertaining to the economic assessment of leak detection methods. Consequently, several important research gaps currently remain in literature:

- No quantitative economic assessments of monitoring strategies for DHS pipelines exist, in particular for TLD.
- The long-term cost implications of pipeline leak growth in DHS networks remain largely unmodelled.
- Economic viability and break-even conditions for advanced leak detection technologies have not been identified.

1.3. Objectives and contributions

This study addresses these research gaps by providing the first economic assessment of TLD for pipeline leak detection in DHS. Focusing on the real-world use case of Central European German-speaking countries, this work makes several novel contributions:

- We introduce and evaluate newly collected empirical data from the most extensively developed area of DHSs in Europe [1].
- Exemplary DHS pipeline leak growth and associated ongoing and repair costs are modelled for the first time, offering insight into long-term impacts of leaks.
- The practical cost for TLD is estimated, with which a first-of-its-kind BEA is performed. With it, key economic thresholds for TLD viability are established.
- Given the findings of both the empirical study and BEA, recommendations are provided for use of TLD and LD in general to help DHS operators in their decision making.

By bridging the gap between technical potential and economic feasibility, this work contributes to the informed adoption of innovative TLD techniques that can improve the sustainability and reliability of DHSs operation. To this end, the paper is organised as follows: After Section 2 details leak detection approaches and the focus on thermography, Section 3 presents the empirical study. The analysis is described in Section 4, while recommendations are derived in Section 5. The study concludes with Section 6.

2. Foundations and methodological context

2.1. District heating and the need for leak detection

DHSs distribute thermal energy from central production units to urban areas via networks of predominantly underground pipelines. Since their emergence in the late 19th century, DHS technologies have evolved through four generations characterised by decreasing temperatures of the utilised heated medium, improved insulation, and the integration of renewable heat sources [26,27]. Today, modern systems predominantly employ pre-insulated pipes (PIPs) with steel carriers, so-called pre-insulated rigid pipes (PIRPs) [28]. A detailed overview of pipeline installation methods and types is provided in Appendix A.

As providers of essential urban heating, DHSs form part of critical infrastructure [29]. Failures can cause severe disruptions and safety risks, as highlighted by outages in Lithuania (2006) [30], Harbin (2020) [31], and even deadly incidents such as in Zhengzhou (2021) [29].

Over time, DHSs face degradation owing to their extreme operating conditions, which include high temperatures, pressure, and humidity [29]. Of all components, pipelines have been found to be the most vulnerable to damage [31,32]. Four years of data from Heilongjiang province, China, show that 56 % of faults originate in pipelines — over 2.3 and 5.5 times more than those linked to valves and compensators, respectively [4]. These failures are attributed to both internal and external causes, including corrosion, installation errors, or environmental exposure [5,32,33]. Among these, external corrosion is most commonly identified as the leading cause [30,34].[1]

If not caused by accidental external damage, pipe failures are usually preceded by micro-damage [35]. The presence of leaks is therefore indicated by the increasing need for water input, so-called makeup water [33]. Even small leaks can cause severe financial losses due to the requirement to chemically and thermally treat additional water and reduction in efficiency [10,35]. Early detection is therefore crucial for reducing operational costs and avoiding major disruptions later on. Given the uneven wear across systems [34], regular, data-driven assessments are essential for prioritising maintenance [35]. To this end, effective LD tools are key to ensuring safe, efficient, and sustainable operations.

2.2. Methods for leak detection

A wide range of methods and tools exist for LD in DHS pipelines. They differ greatly in terms of methodology, technology readiness level, commercial availability, and practical application. LD systems can be dynamic, i.e. the technology involved consists of mobile devices, or static, when sensors are fixed in one place [11]. Various reviews and technical handbooks detail the numerous approaches in existence, ranging from implemented in practice to state-of-the-art [7,10,11,21,28,36–39]. In the context of this paper's Central European region of study, the following list provides an overview of relevant LD methods:

- **Operational monitoring**: Changes in pressure or make-up water demand can indicate leaks [36–38], though they do not allow precise localisation [37].
- **Visual and mechanical-technological methods**: Ranging from expert visual inspection [36] to more complex inspection crawlers, ultrasonic wall-thickness measurements, and moisture metres [11,37], these approaches are effective for assessing specific network sections, though they require direct access to the pipelines [37].

[1] In Yekaterinburg, prolonged water exposure caused 80 % of pipe ruptures [34].

Table 1
Qualitative comparison of district heating LD methods based on pipeline applicability, area coverage, capability, application mode, and operational effort.
Source: Based on descriptions from Arbeitsgemeinschaft Fernwärme [Consortium on District Heating] (AGFW) [37], Gurklienė et al. [36], Heating [28], Latif et al. [11], El-Zahab and Zayed [7], Woods [38] and Konstantin and Konstantin [39].

Method	Pipeline applicability	Coverage		Diagnostic capability			Application mode				Operation effort
		Network-wide	Chosen section	Condition overview	Leak presence	Leak pin-pointing	Fixed	Mobile DC	Mobile IC	Mobile RS	
Operational	All	✓		✓	✓		✓				Low
Visual	All exc. PIPs[a]		✓	✓	✓	✓		✓	✓		Mid
Tracer	All	✓[b]	✓		✓	✓		✓			High
ILDSs	PIRPs only	✓	✓	✓	✓	✓	✓		(✓)[c]		Low-mid
TLDs	All	✓	✓	✓	✓	✓			✓	✓	High
Radar	Buried only		✓	✓	✓	✓			✓		High
Acoustic	All		✓		✓	✓			✓		High

Legend: DC = direct contact (at/in pipe), IC = indirect contact (close proximity), RS = remote sensing.
[a] PIPs indicators exist but are not generally applicable (i.e. steam from close manholes).
[b] Only if areas are not hydraulically separated or blocked [37].
[c] Manual control needs indirect pipeline contact for portable device measurements [28].

- **Tracer methods**: Injected substances, such as Helium, become detectable when the heated medium escapes through a leak, enabling precise pinpointing [7,36,37]. While measurement systems are highly sensitive, the approaches are often operationally complex and expensive [36].
- **ILDS**: PIRPs specifically can be equipped with monitoring wires in the insulation layer to detect moisture ingress [28,37,38], which require correct connection during pipe installation. The most common systems are the Nordic [36] and Brandes [28], respectively, which can implemented for central, decentral, or manual LD [28,37].
- **Thermography**: Heat released into the surrounding environment by a leak can be detected as a hotspot in TIR imagery, allowing for precise pinpointing [6,37]. Image acquisition can occur from ground-based, vehicle-mounted, or airborne (i.e. UAS) cameras [10,36], with the latter offering high flexibility at low cost [15].[2] However, TLD remains sensitive to data quality, and leak identification requires an expert or complementary software [5,11,15].
- **Ground-penetrating radar**: Electromagnetic radiation can be used to examine the subsurface and identify leaks in buried pipes through changed reflected frequencies. While precise, experienced operators, costly equipment, and above-ground access are required. [36]
- **Acoustic methods**: Leak-induced noise can be detected using synchronised acoustic sensors and correlation analysis. While accurate for localisation, they are sensitive to background noise, require above-ground access, and expert handling. [11,37]

2.3. Motivation for methodological focus on TLD

Table 1 provides a qualitative comparison of the afore-described methods. Approaches are contrasted across key operational aspects, including pipeline applicability, spatial coverage, diagnostic capability, application mode, and overall operational effort. In showcasing practical strengths and limitations, it provides context for this study's methodological focus. Among the existing LD techniques, the study prioritises TLD for several reasons. First and foremost, even without the latest advances in automatic image analysis, it is recommended as a viable method by various handbooks [28,33,36] as well as the German Consortium on District Heating [37]. Compared to more proactive static methods, such as ILDS, TLD is not just limited to PIRPs and not wholly reliant upon initial correct installation, but entirely pipeline-agnostic[3] [37]. Where most visual and mechanical-technological methods require direct pipeline contact, the thermographic approach is entirely non-invasive and – via remote sensing – able to reach manually inaccessible areas. Given recent developments in UAS technology and automatic image analysis, the manual and organisational effort associated with TLD is reduced, particularly compared to acoustic and tracer-based methods. While this study's focus lies solely on leak detection and localisation, Arbeitsgemeinschaft Fernwärme [Consortium on District Heating] (AGFW) [37] also highlight TLD's versatility for condition monitoring — and even quality assurance during installation for some pipeline types.

Given the combination of broad pipeline applicability, network-scale coverage, and non-invasive operation as well as the fact that TLD is of yet lacking any form of economic assessment, this scalable and flexible method is selected as the focus of our study.

3. Empirical study

A central part of this study consisted of conducting interviews with DHS operators to gain insight into network management and the occurrence and handling of pipeline leaks in practice. To this end, a case study was developed based on DHS in Central European German-speaking countries, where networks meet around 15 % of heating demand. With record growth rates, Germany alone accounts for more than 34,000 km of trench length, representing the largest share of DHS pipes in Europe [1]. Given their historical development there [27], networks reflect a diverse mixture of pipeline generations and installation methods (see Appendix A). Mirroring global trends, PIRPs are the most dominant pipeline type (Fig. 1.a) [39] and this transition towards newer generations is reflected in the distribution of heat carriers given today (Fig. 1.b) [3]. These characteristics make DHSs from Central European German-speaking countries a particularly relevant region of study for analysing pipeline leaks and their operational implications.

To investigate leak occurrence and management practices within this regional context, 35 network operators from DHSs of various sizes and locations were contacted, of which nine – eight from Germany and one from Switzerland – agreed to participate. The interviews were conducted between January and July 2025 and consisted of a list of survey questions which can be found in Appendix C. While the responses varied greatly in detail as well as quantity, this chapter

[2] Further details on TLD acquisition, including relevant conditions and an illustrative setup and workflow, are provided in Appendix B.

[3] While leaks in duct-based pipes will not cause the heated medium to spread to the surface, they are commonly caused by breaks in the ducts themselves which can be seen in TIRs. Arbeitsgemeinschaft Fernwärme [Consortium on District Heating] (AGFW) [37] presumably highlight its pipe-agnostic applicability for this reason.

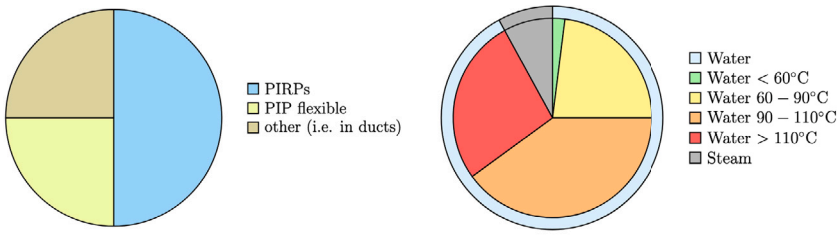

(a) Pipeline installation systems (b) Heat carrier temperatures

Fig. 1. Characteristics of DHSs infrastructure in Germany in 2020 and 2021 [3,40].

Table 2
Characteristics of participating networks, generalised through categorisation into four groups according to their pipeline lengths.

Characteristic				Unit	S	M	L	XL
DHS grid length				km	<30	30–100	100–300	>300
Heat production				GWh/yr	20–45	75–85	300–850	>900
Connected households				–	50–400	1000–5000	20,000–50,000	>50,000
Share heat demand covered by DHS				%	12–13	13–40	12–25	30–90
Avg max flow temperature (as per Fig. 1.b)				°C	90–110 (~100)	>110 (~120)	>110 (~125)	>110 (~132)
Installation method	Above ground			%	0	0	<1	<1
	Underground duct-based			%	0	0	18	20
	Underground ductless	Pour-in-place		%	0	0	<1	<1
		PIP	Glide	%	0	0	<1	<1
			Rigid	%	95	94	70	51
			Rigid (dated)	%	0	0	4	<1
			Flexible	%	0	0	<1	5
			Twin	%	0	6	0	<1
	Cellar pipes			%	0	0	5	8
	Unknown			%	5	0	2	11

summarises the supplied information as best as possible. Where none was provided, slashes ("/") are used to indicate missing data. For the purpose of anonymity, a Roman numeral from *I* to *IX* is associated with each DHS and used to reference each where they are sources of specific information.

To get an overall picture of the currently implemented approaches for DHS LD management, an interview was also conducted with a representative of LANCIER monitoring [41]. The company specialises in infrastructure monitoring worldwide and develops ILDS for DHS in particular for the German-speaking market [G. Roehl, personal communication, May 8, 2025].

3.1. General overview

DHSs in Central European German-speaking countries vary greatly in size — from small local networks of just a few kilometres [G. Roehl, personal communication, May 8, 2025] to some of the largest in the European Union, exceeding 2.000 km of pipeline [42]. To balance the need for generalisability with an accurate portrayal of network diversity, this study's DHSs are categorised into four groups according to their pipeline grid length. This has the additional benefit of preserving participant anonymity. The four-tier categorisation is defined as follows: 1. S ($L_{DHS} < 30\,km$), 2. medium (M) ($30\,km < L_{DHS} < 100\,km$), 3. large (L) ($100\,km < L_{DHS} < 300\,km$), 4. XL ($300\,km < L_{DHS}$).

An overview of general network characteristics is provided in Table 2. Each category is represented by at least two DHSs, for which averages or ranges are provided. Although some initially began as steam-based, all participating networks use hot water as a heat carrier, as is common to DHSs nowadays (see Section 2.1). Various pipeline diameters are installed, ranging from *DN*20 to *DN*500 [*VIII*].

As expected, the heat produced for end use and the number of connected households are closely related to network size. Similarly, maximum flow temperature increases with pipeline length, although – with most temperatures above 110 °C – the participating networks are generally on the higher end of the spectrum of German DHSs (see Fig. 1.b). Given these circumstances, the interviewed network operators may handle potentially more challenging conditions than on average. To better characterise each category, the percentages of pipeline types were averaged to match the installation methods introduced in Appendix A. When it comes to the types of installed pipelines, network size can be seen as an indicator of diversity. Larger networks show much greater variety than smaller ones due to their greater age, as demonstrated by the existence of duct-based systems and other outdated types. S to M DHSs, on the other hand, consist almost exclusively of the newer PIRPs in single or twin form (see Appendix A).

3.2. Leak occurrences

Table 3 gives an overview of leaks and the impact of their occurrence in DHSs. Network losses vary greatly between the different DHSs, though they generally reflect the 10 % identified by Arbeitsgemeinschaft Fernwärme [Consortium on District Heating] (AGFW) [3] as an average for German DHSs. Aside from heat losses [*IV*], leaks constitute a considerable part of these [*I, V, VI*]. As may be expected, the number of leaks per year increases with network size. Although observed leak rate ranges can be calculated using such values (as shown in Table 3), these suffer from detection bias as not all leaks are found and repaired. This problem is particularly prevalent in larger networks, as highlighted by the standard losses some operators were able to provide. In these instances, operators either do not have the resources available to locate the remaining leaks, are currently not able to repair them (see Section 3.3), or do not believe the efficiency increase to outweigh the localisation and repair effort. It may therefore be assumed that true leak rates for larger networks are higher than those in Table 3. Beyond typical loss levels, DHS operators report leaks to cause more than a quadrupling in losses. Even a XL network mentions more than double their already heightened baseline losses to occur before LD and repairs are initiated.

Table 4
Characteristics related to LD of participating networks.

Characteristic			Unit	S	M	L	XL
LD methods	Conventional	Operational change	–	✓	✓	✓	✓
		Public notification	–	✓		✓	✓
		Visual checks	–		✓	✓	✓
		ILDS	–			✓	✓
	Novel	TLD	–	✓	✓	✓	✓
		Acoustic	–		✓		✓
		Tracer-based	–			✓	
ILDS	Installation		%	98	100	58	29
	Type	Nordic	–	✓	✓	✓	✓
		Brandes	–	✓		✓	✓
		Other	–			✓	
	Usage	Not used	–	✓	✓	✓	✓
		Decentral/manual	–			✓	✓
		Central	–			✓	
Leak duration	Days		–	✓	✓	✓	✓
	Weeks		–	✓	✓	✓	✓
	Months		–		✓	✓	✓
	Years		–		✓		

Table 3
Characteristics related to leak occurrences of participating networks.

Characteristic	Unit	S	M	L	XL
Network losses	%	8–16	12	12–25	10–19
Standard losses	m^3/day	/	6	96	480
High losses	m^3/day	/	25	/	960
Repaired leaks	#/yr	≤1	2–4	9–24	60–140
Leak rate ranges	#/km	0.02–0.1	0.05–0.1	0.04–0.1	0.07–0.1
Avg. leak rate	#/km	0.06	0.09	0.09	0.09

Pipeline leaks generally start as hairline cracks before growing to greater sizes [35]. According to practical findings from Fuchs and Frommhold [43], these can range from 1.2 m^3/day to 85 m^3/day. Here, hairline cracks are estimated to cause about 2 m^3/day to 3 m^3/day [*V*], while larger leaks may incur 10 m^3/day [*VI*] or grow further to near 20 m^3/h [*I*]. A leak can culminate in a rupture of 1000 m^3/h [*IX*].

3.3. Leak detection

As hinted at in the previous section, DHS losses vary greatly depending on the implemented monitoring strategy, which tends to align with size-based category. Table 4 summarises the different LD methods used by the interviewed operators, demonstrating commonalities and dissimilarities.

The first indicator of system leaks are changes in operational parameters, such as pressure drops and the requirement for make-up water. While these are monitored by all DHS operators, they cannot reveal the concrete location of a leak. For that purpose, other methods are listed as having been implemented, each with a varying degree of emphasis and priority. For example, several operators stated using calls from citizens as an alert and means of locating leaks. However, a XL network is the only one to indicate that this is the main localisation method they rely upon. Only in the rare cases where no notification is provided and losses are exceedingly high is an active search initiated. While another XL operator describes a much more stringent approach for their smaller secondary networks, they face similar problems in their primary which services half the city. While DHSs of other categories also mention having made use of public notifications, they are generally able to follow a more proactive maintenance strategy by trying to locate leaks of smaller sizes throughout their systems. To this end, visual checks[4] in areas of interest are implemented across the board. Such methods may be useful for sporadic leak localisation, but are not viable as holistic monitoring approaches due to the involved effort. The popularity of their usage highlights a surprising aspect of LD in practice.

Given the prevalence of PIRPs indicated in Table 2, one would expect there to be almost no need for manual methods. In practice, however, the integrated monitoring systems are put to surprisingly little use — paradoxically in particular in S and M networks where their prevalence is highest. The reason provided for this is simple: the operators do not have the (full) circuit diagrams of the monitoring wires and thus lack the capability to interpret the measured results as intended [*I, III, V, VI, VIII*]. Even when plans exist, their usage can still be hampered by wiring errors that occurred during installation [*II, III*] or a lack of personnel [*VI, XI*]. These observations are not just limited to the interviewed DHSs — carelessness during pipeline installation has caused a disuse of integrated monitoring throughout German-speaking countries[5] [G. Roehl, personal communication, May 8, 2025]. However, this is not true for all networks. *IV*, for instance, reported restoring their ILDS recently so that it has now become their main LD and localisation method.

Such examples bring to light a new trend that is mirrored in Table 4, namely a recent focus on monitoring and LD in general. As implied by the previous descriptions and listed repair time frames, several operators show a more laissez-faire approach to leak repair. This contradiction in terms of business economics may be attributed to the fact that many networks, especially S and M ones, originated as a means of using readily available excess heat (such as from incineration plants or production processes) and were not intended or managed as a regular business [*VIII*]. While many operators did not look beyond function fulfilment and network expansion, the energy crisis has placed a new spotlight on DHSs as a means to provide climate neutral heat, causing a change in mindset and interest in a more economical operation [G.

[4] This includes inspecting the ground above pipelines under suspicion to see if they are dry and warm [*V*] or checking for steam rising from manhole covers, which can be an indicator of leaked DHS water heating the sewage system [*I, II*].

[5] The reasons for this are two-fold according to G. Roehl [personal communication, May 8, 2025]. Firstly, if circuit diagrams are not explicitly listed in the installation Statement of Work, they simply are not provided. Reproducing them post-construction is possible, but comes with massive effort and cost. Secondly, very few companies document the circuits with enough precision that they can be used reliably. In Germany, experience has shown only a single company to provide plans of sufficient detail.

Table 5
Causes for leaks with respect to pipeline types (based on data from *II*). All values are given in %.

Component				Share of pipe length [%]	Cause [%]													SUM [%]
					Wear and ageing		Corrosion			Installation and manufacturing errors					External		Unknown	
					Defective component	Leaky component	External corrosion	Crevice corrosion	Steel pipe corrosion	Welding seam defect	Incorrect insulation	Installation error	ILDS defect	Faulty ILDS reading	Construction Damage	Other Damage		
Pipe type	Above ground			1.7	0	0	0	0	0	0	0	0	0	0	0	1.1	0	1.1
	Underground in ducts			12.3	0	1.1	2.1	0	0	0	0	0	0	0	0	0	1.1	4.3
	Underground ductless	Pour-in-place		0.3	0	0	1.1	0	0	0	0	0	0	0	0	0	0	1.1
		PIP	Glide	0.4	1.1	0	5.3	1.1	0	1.1	0	0	0	0	0	0	0	8.6
			Rigid	63.9	1.1	3.2	3.2	0	0	38.3	2.1	3.2	6.4	2.1	4.2	1.1	1.1	66.0
			Rigid *(dated)*	11.2	0	2.1	4.2	0	0	0	0	0	0	0	0	0	0	6.3
			Flexible	0.4	0	0	0	0	0	0	0	0	0	0	1.1	0	0	1.1
			Twin	0	0	0	0	0	0	0	0	0	0	0	0	0	0	0
	Cellar pipes			5.1	0	0	0	0	1.1	1.1	0	0	0	0	1.1	0	0	3.3
	Unknown			4.6	2.1	0	2.1	0	0	0	0	0	0	0	0	0	0	4.2
Other components (flange, compensator)					0	2.1	0	0	0	0	0	1.1	0	0	0	1.1	0	4.3
SUM					4.3	8.5	18.0	1.1	1.1	40.5	2.1	4.3	6.4	2.1	6.4	3.3	2.2	
SUM (by category)					12.8		20.2			55.4					9.7		2.2	

Roehl, personal communication, May 8, 2025]. Given these circumstances, various network operators have reported trying alternative methods, first and foremost among these thermography. This was implemented in various ways, including via aeroplane [*I, IV, XI*], UAS [*II, III, VII, XI*], vehicle-mounted [*XI*], or hand-held sensor [*IV, VI, XI*] — all of which were successful in discerning leaks and their locations. *XI* in particular report having incorporated all forms of thermography into their network monitoring strategy. Information obtained through TIR acquisition flights is mentioned as particularly useful, having helped identify leaks that accumulated to 40 % of network losses [*XI*].

Other reported methods include acoustic techniques, such as the unsuccessful use of correlators by an M network. One XL DHS reported using an ultrasonic listening probe, though they stressed the sensor's ineffectiveness in urban environments given interfering ambient noise. Another XL network reported the continuous use of Uranin-based tracer dye, which is generally helpful to differentiate leaks when they occur at construction sites or near water distribution networks.

As indicated, the duration for which leaks persist in practice depends greatly on the urgency of the situation, expressed in terms of the relative increase of network loss they cause. This in turn is dependant on leak and DHS size. Once leaks reach extreme magnitudes, as those listed at the end of Section 3.2, they are quickly identified due to the disruption they cause in the system [*I*]. They will commonly show visible signs of damage, which are called in by the public [*I*]. Smaller networks may act accordingly for objectively smaller leaks, as they generate a comparatively high relative increase in their network losses. Similarly, losses of the same magnitude might be viewed as irrelevant by XL DHSs who contend with much higher standard losses. Network loss increases that do not warrant the same urgency and immediate attention may persist for much longer time frames. The duration of their existence can be divided into two parts: 1. the time for leak localisation, 2. the time until the repair can be made. The first depends mainly on the maintenance strategy implemented by the DHS operators. If no active monitoring method is used, leaks may not be found for several months or even years [*V*]. The second is subject to the individual circumstances of each situation. Leak repair may be impeded by the following:

- Time of year (i.e. in winter, the need to maintain operational integrity and high flow temperatures may prevent proper repairs [*II, VI*]),
- Location (i.e. areas that are difficult to access or require specific authorisation, such as under airports or railway lines [G. Roehl, personal communication, May 8, 2025]),
- Unavailability of required materials or services (i.e. special filling or wrapping materials [G. Roehl, personal communication, May 8, 2025]),
- Customer requirements (i.e. manufacturers may require process heat for long processes [G. Roehl, personal communication, May 8, 2025]).

Depending again on the urgency of the situation, a temporary fix may be performed to bridge the time until conditions allow for a complete repair [*II*].

3.4. Causes for leaks

As discussed in Section 2.1, the reasons why leaks occur are varied, with corrosion mentioned as the main factor by many studies in literature. Thanks to a detailed breakdown provided by *II* for the years 2019 to 2024, Table 5 can give an overview of the prevalent causes and most affected pipeline types in an exemplary German DHS consisting of various different pipeline types. Interestingly, corrosion is only the second most common cause, with installation and manufacturing errors being the source of more than half of all repaired leaks. Among these, welding seam defects are most prevalent.

A closer look reveals the source of this to be the PIRPs, which seem disproportionately affected.[6] While 66 % of leaks throughout the provided 6 year time frame occurred in these most common of pipelines, 79 % of them were caused by installation and manufacturing errors. This observation coincides with reports made by other interviewed DHS operators that mention such errors as a dominant reason for repairs to become necessary long before the officially estimated end of lifetime[7] [*I, III, IV, V*]. In earlier years, this was attributed to underdeveloped sleeve technology and substandard steel quality from the postwar years, although these aspects have become less problematic

[6] *II* report leaks in these pipes to make up between 58 % to 92 % of yearly occurrences.

[7] The technical service life of PIRPs in Germany is estimated at 36 yrs to 70 yrs, on average 51 yrs [44].

since the 1990s [*I, IV*]. Current errors are assumed to be the result of construction defects and inadequate site supervision [*II, III, V*]. Incidentally, *II* report up to 40 % of annual leaks (to which such errors are counted) still occur within the warranty, customarily a period of 5 years [G. Roehl, personal communication, May 8, 2025]. Other operators such as *VI* also describe the occurrences of multiple leaks annually starting just over 10 years after initial installation. It may be for these reasons that operators such as *VII* go as far as to refute the correlation between pipeline age and occurrence entirely. The fact that these circumstances can be observed across all interviewed DHS operators further underlines the need for active LD.

Table 5 also shows other interesting aspects. External damage causes a comparatively small amount of leaks, about 10 % throughout the regarded time frame. Older systems, such as duct-based and dated PIRP installations are significantly less fault-prone than the previously discussed newer types. Leaks in these pipelines are caused only by corrosion or otherwise wear. This coincides with observations made by other operators, who attest to their general reliability as long as certain conditions are upheld — in particular ensuring the pipe surroundings remain dry [*III, IV*].

With regard to other installation methods not represented in *II*, twin pipes are reported by *V* to be particularly fault-prone. The high flow temperatures are found to induce mechanical stresses that lead to the crack formation and growth, a process often exacerbated by production errors [*V*]. This practical experience contradicts literature such as Mazhar et al. [45], which suggest "to use twin-pipes wherever applicable since their performance to price ratio is the best".

Aside from these pipeline type-related aspects, some general observations regarding DHSs and leak causes should be mentioned. While the main focus often lies on the heating period and operation at high temperatures, difficulties may arise owing to the longer periods of colder flow temperatures. It can cause damage to the installed press technology or sleeves to loosen given the shear forces that occur when the pipe contracts [*V*]. Maintenance is also a key aspect to prevent leak-enabling circumstances. Without it, draining and venting can be compromised, shut-off valves clogged, or salt and water enter the shafts [*V*]. This, again, emphasises the necessity for active LD.

4. Economic analysis

4.1. Estimating leak costs

The cost incurred by DHS leaks can fundamentally be divided into two parts: 1. ongoing, namely the cost of treated and heated make-up water required to compensate for the incurred loss, and 2. one-time, namely the costs of repair. As highlighted in Section 2.1, the longer a pipeline leak remains undetected, the greater the risk of rupture and destruction of surrounding infrastructure [35], a result of which would be very high repair costs. Economically speaking, an earlier detection has the benefit of minimising the considerable ongoing costs DHS operators have to bear while a leak persists [35]. However, both types of cost are difficult to quantify given their dependence on the unique circumstances of each DHS. Nevertheless, this study makes an effort to estimate them given a combination of theoretical sources and practical knowledge from the conducted surveys described in Section 3.

4.1.1. Ongoing costs

Leaks incur ongoing costs chiefly due to the make-up water that must be fed into the system to counteract the ensuing loss. This mainly stems from the required heating and treatment of the water before it can enter the pipelines [35]. The latter is essential to prevent internal corrosion and includes the removal of particulate matter, hardness minerals, salts, and oxygen, as well as addition of chemicals to raise the pH level, stabilise hardness, and prevent particle coalescence [28,38]. The addition of make-up water is outsourced to the DHS water carrier providers, meaning that operators pay according to their individual contracts and circumstances [*V*]. Most interviewed operators were unable to provide costs per cubic metre, indicating that these expenses are not taken note of as carefully as one might expect. *IX* mention 7 €/m^3 as a value from another German DHS, while *V* provide an estimate of 5 €/m^3 for their network with 125 °C flow temperature. *VIII* report a precise value 5.20 CHF/m^3, equivalent to approximately 5.60 €/m^3, for their 20 °C colder network. Following a conservative approach, 5 € is assumed as the cost $C_{make-up}$ incurred per cubic metre of make-up water.

The amount of required water depends on the size of the leak, which in turn depends on the duration of its existence (see Section 2.1). As discussed in Section 3.3, size varies greatly depending on all manner of influencing factors. However, for the purpose of this study, a simplification must be made to quantify ongoing monetary losses. To this end, an exemplary leak and its growth are modelled. While there is a significant lack of literature in this field for DHS pipelines, leak growth models have been developed for those of water distribution networks, which share the same medium and similar characteristics. Specifically, Guo et al. [46] compared different growth functions, including Logistic, Gompertz, and Richards, to identify which is most adept at simulating a leak's growth based on a real leak dataset. They find that the Richards function performs best, which is generally defined as

$$f(t) = \frac{a}{\left(1 + e^{(b-c\cdot t)}\right)^{\frac{1}{N}}} \tag{1}$$

where $f(t)$ is the leak flow rate (m^3/h), t defines the leak duration, and a is equal to the maximum leak flow rate. The other parameters – b, c, and N – are tuned to best simulate the real-world dataset. Guo et al. [46] performs these optimisations for diameters $DN100$ to $> DN400$ and different pipe materials such as cast iron, cement, and steel. The growth coefficient, c, is found to be best defined as 0.20 throughout. The position of the inflection point, b, and the curve steepness, N, are defined by the diameter: $b = 3$ and $N \approx 0.8$ for $\leq DN300$ and $b = 1$ and $N \approx 0.2$ for $> DN300$. a generally grows with diameter and is smaller for steel pipes than cast iron [46].

An exemplary leak is modelled on the basis of the theoretical and practical information described in Section 3. To this end, Guo et al. [46]'s function definition is adapted to the circumstances of this study and to account for the differences between water distribution networks and the systems at hand.[8] To better suit the time frames for DHS leaks (s. Section 3.3), growth is measured in m^3/day instead of m^3/h. The inflection point position b is based on larger pipe diameters with a value of 1. A low growth coefficient c of 0.01 is selected to reflect much longer leak progressions, while the curve steepness of $N = 0.4$ similarly allows for a gradual S-curve. The maximum leak flow rate a is selected as 30 m^3/day to simulate the following behaviour: The leak starts as a small hairline crack of 1 m^3/day [43], a more conservative choice than the reported 2 m^3/day to 3 m^3/day [*V*]. It reaches 10 m^3/day after 6 months, equivalent to a leak of a somewhat larger size [*VI*], and arrives at 20 m^3/day after a year, thereby equating the additional network losses reported by M networks. Although the modelled leak does increase progressively over time, in an effort to balance out the possible extremes, it stays well below the more major occurrences reported in practice and literature. It therefore simulates a leak that will not necessarily be called in by the public.

The leak growth curve can be translated into cost via Eq. (2). The cumulative summation helps obtain an amount in cubic metres for a given number of days that the leak exists, while multiplication with the cost of make-up water $C_{make-up}$ translates to a quantification of economic value attributable to the ongoing loss. For the exemplary leak growth shown in Fig. 2, the cost can be defined as a function of time —

[8] Specifically, DHSs have a significantly higher medium temperature to fulfil their purpose, which necessitate other pipe materials.

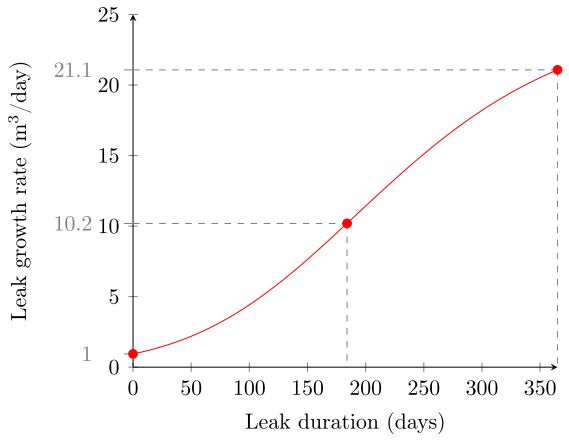

Fig. 2. Leak growth of an exemplary leak with a =30 m³/day, b = 1, c = 0.01, N = 0.4.

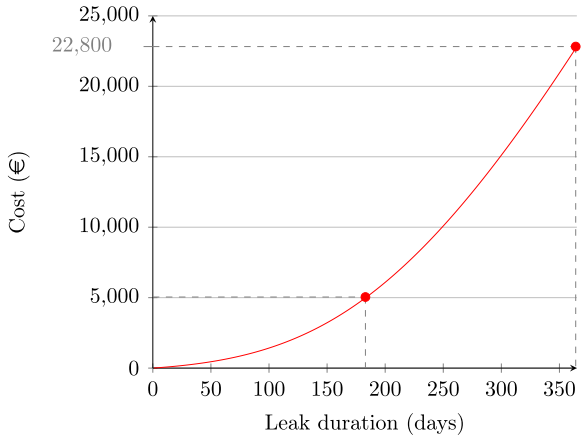

Fig. 3. Cumulative ongoing cost of the exemplary leak defined by Eq. (3).

specifically leak duration (s. Eq. (3)). The cumulative cost is visualised in Fig. 3.

$$C_{\text{ongoing}}(t) = C_{\text{make-up}} \cdot \sum_{t=0}^{T} f(t) \tag{2}$$

$$C_{\text{ongoing}}(t) = 5\ \frac{€}{\text{m}^3} \cdot \sum_{t=0}^{T} \left(\frac{30\ \frac{\text{m}^3}{\text{day}}}{\left(1 + e^{(1-0.01\cdot t)}\right)^{\frac{1}{0.4}}} \right) \tag{3}$$

4.1.2. Repair costs

Beyond the costs incurred while leaks persist, additional expenses arise from repairs. On this aspect, the interviewed DHS operators were able to provide significantly more detailed information than they could about ongoing losses. In general, repairs may consist of several cost categories, such as those for materials, civil engineering work, pipe construction, welders, construction cite coordination, and traffic re-routing [*II, V*]. The required services are commonly outsourced to specialised companies [*V*].

The precise requirements are unique to each leak and costs can vary greatly depending on a multitude of factors, such as the surrounding infrastructure, pipeline installation method, cause of failure, time of occurrence relative to the heating period, and many more. Repair costs registered by the participating DHSs described in Section 3 spanned an incredibly broad spectrum from 2000 € to over 1,000,000 €. In general, the more complex the circumstances, the greater the expense [G. Roehl, personal communication, May 8, 2025]. As Table 6 shows, such

Table 6
Estimated cost ranges for a single leak repair.

Characteristic	Unit	S	M	L	XL
Repair cost	€	5000–250,000	3500–100,000	2000–> 1,000,000	avg. 25,000; mostly <100,000

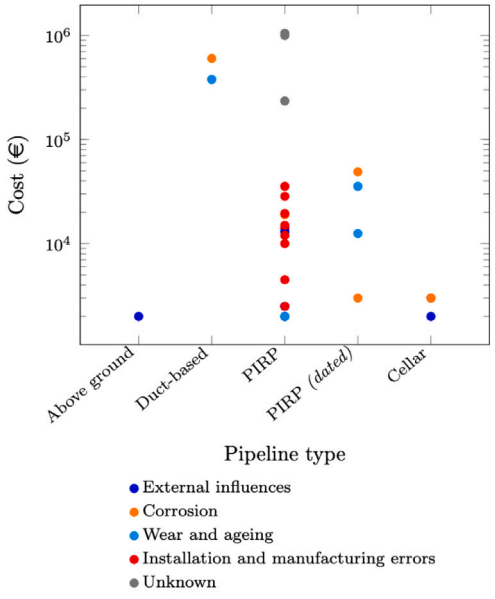

Fig. 4. Repair costs for leaks reported by *II, III, VIII*.

complicating conditions have occurred in DHSs of all sizes, given their placement in urban, and thus structurally speaking complex, areas.

The relationship between leak repair costs, their cause, and affected pipeline type is displayed in Fig. 4, largely thanks to a detailed breakdown of occurrences throughout 2024 provided by *II*. Despite the comparatively small number of data points and thus arguable statistical relevance, some important observations can be gleaned from it. Similarly to Section 3.4, the figure highlights the prevalence of leaks in the most common form of pipelines (PIRP), mainly on account of installation and manufacturing errors. The repair costs for this pipeline type also spans the greatest breath, from 2000 € to 1,000,000 €. Even PIRP leaks attributed solely to installation and manufacturing errors can range from 2500 € to 35,000 €, highlighting again the relevance of situational circumstances. Unsurprisingly, leaks in underground pipelines are more expensive than above-ground or cellar variants. Duct-bound pipes, in particular, require high repair cost due to the nature of the installation method [*II*]. Aside from this, leaks caused by corrosion seem to generally cause greater expenses than wear and ageing or external influences.

Several DHS operators highlight a correlation between the duration for which a leak exists and its repair cost. For PIRPs, *V* list smaller leaks to require 3000 € to 8000 € for civil engineering and 500 € for materials (mainly sleeves), but these costs increase for leaks that exist for longer time frames to a total of around 20,000 €. This is because material costs escalate to 3000 € to 4000 € when re-insulation becomes necessary due to a larger leak size. These numbers showcase how fixing leaks earlier can save between 1.7 to 5.7 times in repair costs. Similarly, costs of extreme magnitudes of >1,000,000 € often stem from infrastructure damage caused by the prolonged existence of leaks [*III*]. *III* list two such events in which entire crossings or network sections needed replacing due to 6 months of persistent moisture leakage.

To quantify exemplary repair costs for this economic analysis, several assumptions and generalisations must be made. PIRPs are considered for the example leak due to their current and future prevalence

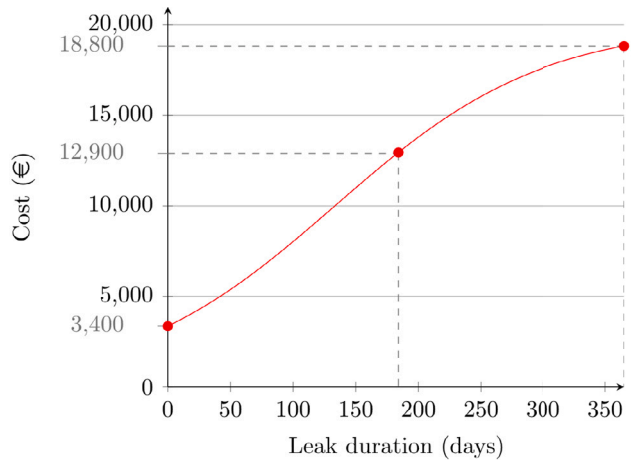

Fig. 5. Repair cost growth of an exemplary leak defined by Eq. (5).

and high occurrence both in the given DHSs (Section 3.1) and leak statistics (Section 3.4). The key information provided by *V* on the effect of leak duration on repair costs is used as reference to model the time-based dependence. As per *I*, repair costs commonly do not exceed 100,000 €, meaning instances above these are viewed as outliers and not considered for our conservative example leak. Taking into account the remaining values shown in Fig. 4, the repair cost for a leak of this pipeline type averages at around 12,900 €. This is close to the average of the reported range by *V* for longer existing leak repairs, namely 13,000 €. We therefore assume this to be the cost for repairs after 6 months. The starting point is selected using the average of lower repair costs reported by different operators for PIRPs. These encompass the cluster of instances of lower repair costs from Fig. 4 – that average to 2700 € – as well as lower bounds of various provided value ranges, including 3500 € [*V*] and 5000 € [*VI, VII*]. Together, these combine to an average of around 3400 €, close to equal to the lower bound of the fast repair range defined by *V*. To approximate the extent of the duration-induced cost increase, the repair expenses after a year's existence are also estimated. The cluster of higher leak repair costs from Fig. 4 amount to an average of 18,500 €, just short of the 20,000 € value defining the upper bound of the slower repair range [*V*].

Given these data points, a function is defined to model the time-based cost progression of leak repairs. As simpler functions (such as linear, exponential, or logarithmic) are not able to properly capture the described circumstances, a growth function similar to the one from Section 4.1.1 is chosen. For the given purpose, we select the simplest and most well-known sigmoid function, the Logistic function [46,47], generally defined as in Eq. (4).

$$C_{\text{repair}}(t) = \frac{a}{\left(1 + e^{(b - c \cdot t)}\right)} \tag{4}$$

Here, the maximum cost a is defined as the upper bound 20,000 €. The remaining parameters, b and c, are chosen as 1.6 and 0.012 respectively to fit the function to the circumstances. This results in a time-dependent repair cost progression as defined by Eq. (5) and shown in Fig. 5.

$$C_{\text{repair}}(t) = \frac{20{,}000\,€}{\left(1 + e^{(1.6 - 0.012 \cdot t)}\right)} \tag{5}$$

4.1.3. Total leak costs

The ongoing and repair costs from Sections 4.1.1 and 4.1.2 can be combined into total leak-induced costs by summation. Fig. 6 displays the resulting cost for the derived exemplary leak, for which a conservative growth and repair were estimated. For any point in time t, the plot shows the cost that the leak accumulated throughout its lifetime, were it be repaired that day. Although repair costs make up the lion's share of expenses in the beginning, the figure clearly shows how ongoing costs replace these in severity if the leak persists for long enough (e.g. contributing more than 50 % after 1 year). It is important, therefore, that these costs are not underestimated.

A combined SA of the fixed-value ongoing and repair cost assumptions is provided in Appendix D. It shows that plausible lower- and upper-bound parameter choices affect the magnitude of cumulative leak cost, but not the qualitative finding that C_{ongoing} becomes the dominant component for sufficiently long leak durations. Across all tested scenarios, this happens within the first year of a leak's existence, with the parity point occurring as early as 249 days when make-up water is valued at 7 €/m^3. This indicates that the strategic importance of rapid leak repair is not merely a product of the baseline assumptions, but a fundamental characteristic of this kind of leak cost modelling.

4.2. The economic necessity for alternative LD methods

In terms of economic viability and cost efficiency, the interviews with DHSs operators also highlight a current need for alternative LD techniques despite commonly installed ILDS or use of other traditional methods. This can be attributed to the following:

1. Lack of usability: ILDS either do not exist or have not been installed in a way that allows them to be used (incorrect wiring, missing circuit diagrams) [*V, VI, VIII*].
2. Lack of usage: Systems are not used as required, i.e. manual readings are not performed regularly. For *III*, this caused a leak to go undetected for 6 months, culminating in 1,000,000 € repair cost.

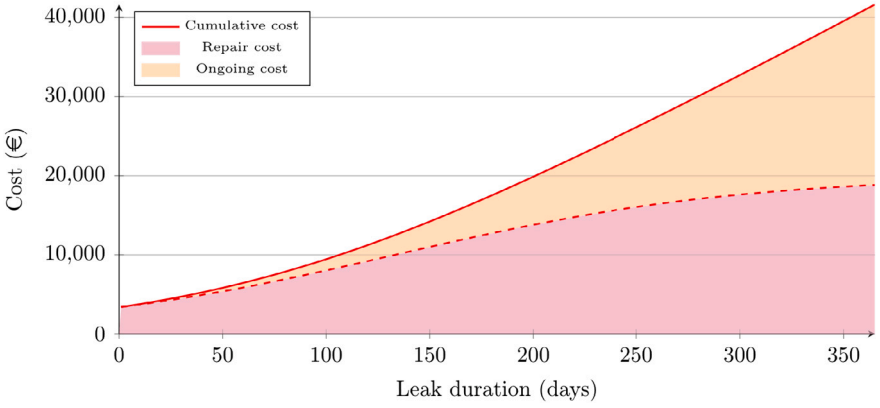

Fig. 6. Combined cumulative ongoing and repair costs for an exemplary DHS leak.

3. System malfunction: The ILDS either does not give a warning despite the presence of a leak, returns a false positive or provides an incorrect location. The first caused *III* to fail to localise a leak for 6 months, again causing costs of 1,000,000 €. The second can lead to unnecessary excavations and cost, such as for 2500 € as described by *II*. Incorrect localisations are attributed with 1000 €/m by *I*, though examples show they can grow to over 2000 €/m[9] [*VIII*].

These aspects call into question the advisability of relying solely on ILDS. As described in Section 3.3, the monitoring strategies shown by DHS operators in practice seem to reflect similar conclusions, with many of them turning to a combination of methods and alternative options, such as thermography.

4.3. Estimating TLD costs

The usage of TLD for DHS incurs its own cost, which is quantified in this subsection. However, the method as described in Section 2.2 is characterised by some factors that require consideration for cost estimation. Mainly, these consist of the time frame limitation and the form of acquisition itself.

Given the stringent requirements for TIR acquisition discussed in Section 2.2, the time frame for data collection is limited. This naturally sets boundaries for the applicability of the method and must therefore be quantified as part of the economic viability assessment. By means of a comprehensive analysis of historical weather data in Germany, included in Appendix E, the viable number of days per year in which TIRs can be acquired is estimated as 40. Clusters of days at the beginning (November), middle (January), and end (March) of the heating period are found to commonly exhibit suitable characteristics that allow the capture of high-quality images, meaning multiple acquisitions per year are theoretically possible.

While the technology can be implemented via ground-based (hand-held, vehicle-mounted) or aerial (UAS, aeroplane) sensor, practical experience has shown the latter to be most viable. Ground-based thermography allows for the highest ground sampling distance (GSD) but at the cost of an extremely time-consuming acquisition.[10] Additionally, these methods are subject to access restrictions in many urban areas, preventing full coverage [*IX*].

The most suitable type of aerial acquisition is a matter of contention among the interviewed operators. While *IX* have incorporated aeroplane-based TLD into their monitoring strategy, *IV* report images from this form of acquisition to provide only superficial overviews and not enough detail for comprehensive LD. This is due to the lower GSD, a side effect of the great flight heights. In comparison, UASs can fly much closer to the ground,[11] thereby combining the benefits of high resolution and full coverage in one. At the same time, Heipke and Tödter [48] state around 20 km of pipeline can be covered via UAS per night, making it 10 times faster than the hand-held approach. While this speed may not be sufficient to cover of the largest XL networks in their entirety, its flexibility and applicability to most forms of network make UAS-based acquisition the main focus of this study.

The cost of UAS-based thermography comprises several key elements. These include the hardware (thermal camera and UAS), the acquisition flights (trained pilot), and the evaluation of the data (expert image analysis). While it is theoretically possible for operators to invest in the required technology and train or hire expert staff, this would mean a substantial initial investment. In terms of hardware, the costs are driven by thermal sensors, which are considerably more expensive than standard colour cameras [49].

As an alternative, several companies in Germany have begun offering the UAS-based thermography as a package service. In an effort to find specific leaks in their networks, some interviewed operators report trying such services. They list expenses of between 300 and 600 €/km for network coverage [*VI, VII*]. To further disaggregate these costs, offers were requested from different companies for an exemplary region. Three areas of expense are thereby identified: 1. flight costs C_{flight} (20 % to 30 %), 2. operational expenses $C_{\text{operation}}$, ranging from travel and accommodation to generators for loading the UAS batteries (30 % to 60 %), and 3. image analysis effort C_{analysis} to identify leak candidates for report creation (25 % to 40 %). For comparison, in the case of aeroplane-based acquisition – which is listed by *IX* as costing 143 €/km – roughly 50 % are attributed to image analysis and report generation.

Recent advances in the field of TIR analysis for DHS LD have enabled the automation of said analysis step [6,9,14,15,17,18,48]. This not only allows for the reduction of a considerable portion of service cost for both kinds of aerial acquisition, but also removes the time-related bottleneck meaning results can be provided faster to the operators. Additionally, it may supply DHS operators with the necessary tool to implement the approach themselves by eliminating the requirement for extensive thermographic knowledge.

Taking all afore-mentioned aspects into account, the cost of UAS-based thermography as a service can be quantified in general according to Eq. (6), with n_{service} the number of DHS flyovers planned per year, C_{service} the service cost per km, and L_{DHS} the network pipeline length:

$$C_{\text{TLD}} = n_{\text{service}} \cdot C_{\text{service}} \cdot L_{\text{DHS}} = n_{\text{service}} \cdot (C_{\text{flight}} + C_{\text{operation}} + C_{\text{analysis}}) \cdot L_{\text{DHS}} \tag{6}$$

Assuming the average of expenses reported by DHS operators, the cost to requisition UAS-based TLD C_{service} is defined as 450 €/km. However, since the analysis step can be automated, the associated cost C_{analysis} can be eliminated, thus reducing the total TLD cost. Given the previously described range for C_{analysis}, C_{service} can drop to 270 €/km to 337.5 €/km. For the purpose of this study, the most conservative value is chosen — meaning 25 % savings. The TLD costs can therefore be summarised as shown in Table 7 for this study's four-tier categorisation (see Section 3.1). Given the average number of viable days for TIR acquisition per year and kilometres of pipelines that can be covered by night, all sizes of DHS (up to 800 km) can be checked via UAS-based thermography at least once per heating period ($n_{\text{service}} = 1$). The TLD cost is therefore a function of DHS length and defined as Eq. (7).

$$C_{\text{TLD}}(L_{\text{DHS}}) = 1 \cdot 337.5 \ \frac{€}{\text{km}} \cdot L_{\text{DHS}} \tag{7}$$

Table 7
Estimated cost ranges for the TLD approach.

Characteristic	Unit	S	M	L	XL
L_{DHS}	km	<30	30–100	100–300	>300
C_{TLD}	€	<10,110	10,110–33,750	33,750–101,250	>101,250
Required time frame	nights	≤2	2–5	5–15	>15

4.4. Break-even analysis

The previously estimated costs of exemplary leak and TLD are compared to assess the economic viability of the latter method. In particular, the objective of the analysis lies in identifying the BEP for TIR-based DHS pipeline LD. To this end, the following scenarios are contrasted in a BEA:

$$TC_{\text{inf}} = n_{\text{leaks}} \cdot \lim_{t \to \infty} C_{\text{ongoing}}(t) \tag{8}$$

[9] An instance of incorrect localisation reported by *VIII* lead to a tripling of repair costs when 30 m of pipeline required excavation until the true leak position was pinpointed.

[10] According to *VI*, the hand-held approach takes around 4 h/km, meaning that only around 2 km can be covered in one night.

[11] Sledz and Heipke [17] achieve a GSD of 5.2 cm for their UAS flight at 40 m, representing nearly a 5-fold improvement in resolution compared to the 24 cm GSD reported by Friman et al. [6] for their 800 m aeroplane flight.

Table 8
Network characterisations for break even analysis.

Characteristic		Unit	S	M	L	XL
General	L_{DHS}	km	0–30	30–100	100–300	300–800
	Leak rate	#/km	0.06	0.09	0.09	0.1
	n_{leaks}	#/yr	0–2	2–9	9–27	30–80
Example	L_{DHS}	km	17	56	200	550
	n_{leaks}	#/yr	1	5	18	55
	t_{TLD}	nights	1	3	10	28
	$t_{d_{min}}$	days	8	10	17	35

$$TC_{none} = n_{leaks} \cdot \left(C_{ongoing}(T) + C_{repair}(T)\right) \quad (9)$$

$$TC_{TLD} = n_{leaks} \cdot \left(C_{ongoing}(t_d) + C_{repair}(t_d)\right) + C_{TLD}(L_{DHS}) \quad (10)$$

In the reference scenarios (Eqs. (8) and (9)), leaks are not actively sought, meaning no expenses are incurred by detection methods. Instead, leaks are assumed to grow — either infinitely (Eq. (8)) or until day T when, for instance, the DHS operators are informed about their location by the public (Eq. (9)). This means they continuously incur time-dependent ongoing $C_{ongoing}$ and – in the case of TC_{none} – repair C_{repair} expenses once found. The costs are combined as discussed in Section 4.1.3. In the TLD scenario (Eq. (10)), leaks are localised via UAS-based thermography. Here, ongoing and repair costs only increase until the leaks have been removed on day t_d, though at the additional price of the thermography-based survey C_{TLD}. At minimum, t_d consists of the number of nights required to survey the DHS – which depends on network size – and the time needed for image analysis and leak repair. The latter duration is estimated at 7 days, assuming the analysis is automated.

The number of leaks n_{leaks} that we assume occur for the purpose of this analysis depend on the size of the network. To quantify this number, the four categories of DHS length are viewed individually. Table 8 presents the defining characteristics for the BEA based on findings from Section 3.2 as well as the following additional assumptions. XL networks are capped at 800 km, as this is the upper limit for a TLD coverage within the viable amount of days (see Section 4.3). Given the detection bias discussed in Section 3.2, we assume a leak rate that increases slightly with DHS size from 0.06 leaks/km to 0.1 leaks/km. While this amplifies the empirically found value for XL networks, it still works conservatively, as we may assume a much higher unrecorded leak number given standard losses in such systems. Combining network size with leak rate provides estimates for a range of n_{leaks} in each system.

Using the thus determined general value ranges, a representative DHS is defined for each of the four network categories (see Table 8, "Example"). In each case, average values for L_{DHS} and n_{leaks} are selected. The former helps define the number of nights required for TLD, t_{TLD}, which in turn helps to estimate a minimum $t_{d_{min}}$. Physical network characteristics such as flow temperature are defined as in Table 2, thereby fulfilling the detection requirements for TLD.

Comparative cost plots for each of the four network categories are provided in Fig. 7. To improve interpretability, it is assumed that all leaks occur simultaneously and that in thermography scenario the C_{TLD} expense is incurred at the beginning — regardless of when exactly the flights take place. As the analysis is focused on a comparatively short time frame and TLD is modelled as a third-party service, factors such as capital investment, discounting, and depreciation are excluded. The figure visualises the BEA for leak localisation and repair at $t_d \in \left\{t_{d_{min}},\ 30,\ 91,\ 183,\ 274,\ 365\right\}$ days, thus spanning from weeks over quarter-year increments to a year. These time frames take into account that delays can occur during localisation (as TLD is only implemented once a year) or repair (see Section 3.3). For reference, the precise values visualised in Fig. 7 are provided in Appendix F.

A comparison with the reference scenarios shows that, regardless of network size or leak removal date, the BEP t_{BEP} is reached in a surprisingly short period of time after t_d – for TC_{none} no longer than three months. Even if one assumes that leaks are never found (TC_{inf}), the extra expense of TLD and repair is shown to always pay off in less than three quarters of a year after t_d.

When comparing the different t_d values, an interesting trend can be observed mirrored through all network sizes. Faster leak detections and removals take slightly longer to amortise than slower ones, specifically the delta $\Delta t_{BEP} = t_{BEP} - t_d$ diminishes with larger t_d values. This is caused by the non-linearity of both $C_{ongoing}$ and C_{repair}, which means that the relative effect of the added constant C_{TLD} decreases over time. For $t_{BEP_{none}}$, for instance, the delta in S networks decreases by 55.4 % from the initial 92 days for $t_{d_{min}}$ to 41 days for $t_d = 365$. This aspect can be seen as favourable for TLD, as one may assume that the probability of a leak being localised by other means (such as public notification) grows over time. Later localisation via TLD should therefore amortise faster for the method to remain viable.

Another interesting observation from Fig. 7 is that TLD pays off faster with increasing network size. This may, in particular, be attributed to the associated leak rates. For instance, XL DHSs have $\Delta t_{BEP_{none}}$ values that range from 52 days ($t_{d_{min}} = 35$) to 25 days ($t_d = 365$), which are 43 % and 39 % smaller, respectively, than those previously listed for S networks. This indicates that the method becomes more viable with higher leak rates.

These findings have an impact on the economic viability of TLD in general. In the best-case scenario, where leaks can be removed in the shortest time frame ($t_d = t_{d_{min}}$), amortisation of the UAS-based TLD service cost takes no more than 3 months after leak removal and the additional repair costs are paid off in less than three quarters of a year. In the worst-case scenario, where leaks are located and repaired only after a year ($t_d = 365$), the cost for TLD is amortised almost within a month after t_d and the entire localisation and repair via TLD pays off in less than half a year after t_d. In summary, this means that the true economic benefit of TLD, namely faster amortisation over time, complements its methodological strength as a LD method, where its advantage lies in the ability to help locate leaks that are otherwise not pinpointed quickly.

The robustness of these findings with respect to cost modelling assumptions is assessed in Appendix G. Although the resulting amortisation periods shift under lower- and upper-bound leak cost scenarios, the qualitative conclusion remains unchanged: TLD continues to amortise within a comparatively short period after leak removal.

In the context of this BEA, an additional SA is performed to show the impact of automation on TC_{TLD}. As detailed in Appendix H, the analysis shows that automating $C_{analysis}$ – and thereby reducing TC_{TLD} by a given percentage – leads to a reduction in the amortisation period Δt_{BEP} by at least the same percentage. This means that even a conservatively estimated automation significantly shortens the amortisation time beyond the savings percentage. Given future technological advancements and growing UAS market [50], this aspect can be expected to provide an even greater potential for cost savings and increased amortisation, as the share of C_{flight} can be expected to drop.

An aspect that is disregarded in this direct cost comparison (as it is not easily quantified) is the additional benefit afforded by the investment in TLD. Acquired TIR images can be used beyond mere LD to assess the condition of the DHS pipelines [*IV, IX*]. If flights are performed regularly, a temporal analysis can provide valuable information on network degradation [14]. *IX* highlight these aspects as other main motivators for using aerial TLD.

5. Recommendations

In light of the findings from Sections 3 and 4, several important statements can be made regarding DHS LD and specifically TLD from an economic standpoint. These elicit general as well as DHS-unique recommendations.

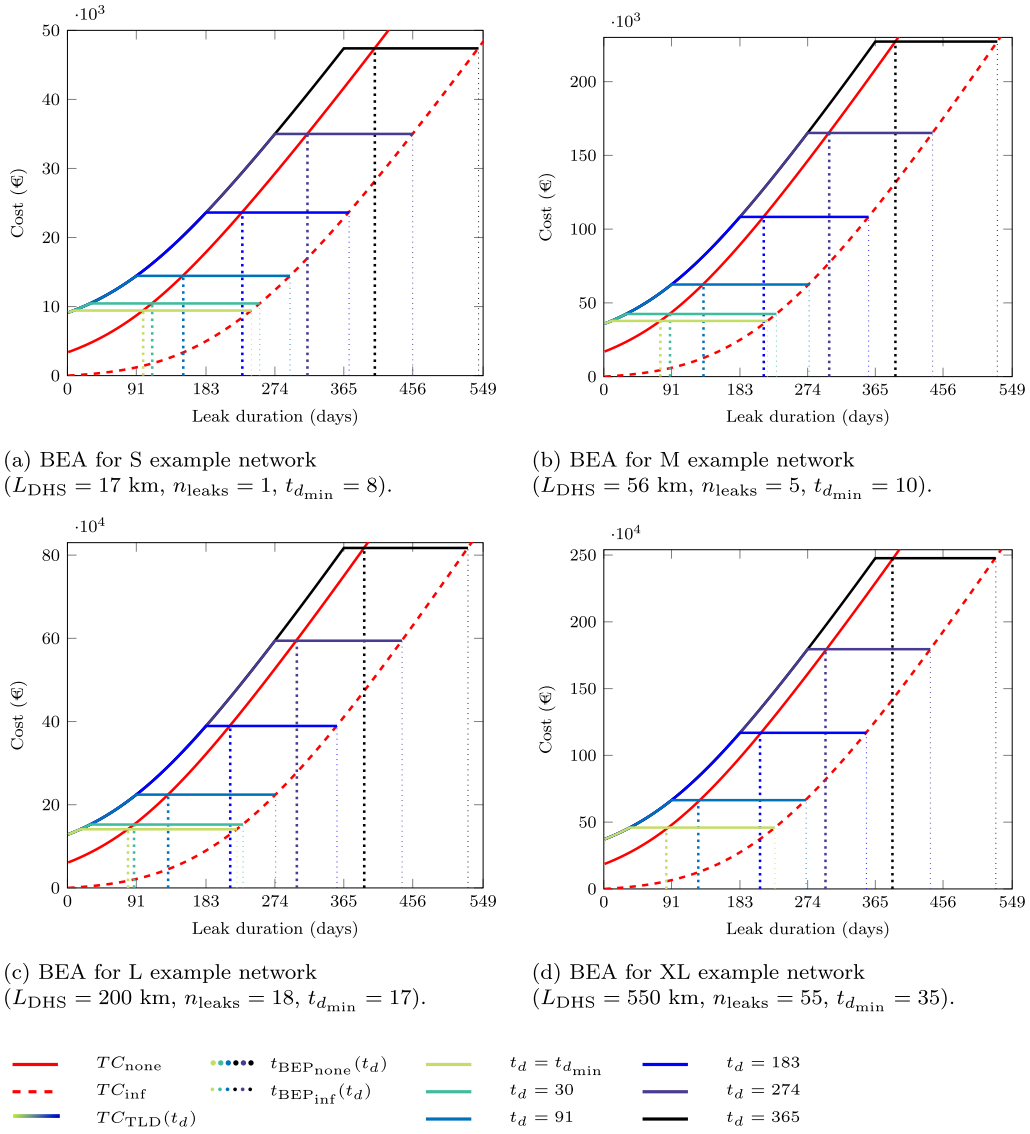

(a) BEA for S example network ($L_{\text{DHS}} = 17$ km, $n_{\text{leaks}} = 1$, $t_{d_{\min}} = 8$).

(b) BEA for M example network ($L_{\text{DHS}} = 56$ km, $n_{\text{leaks}} = 5$, $t_{d_{\min}} = 10$).

(c) BEA for L example network ($L_{\text{DHS}} = 200$ km, $n_{\text{leaks}} = 18$, $t_{d_{\min}} = 17$).

(d) BEA for XL example network ($L_{\text{DHS}} = 550$ km, $n_{\text{leaks}} = 55$, $t_{d_{\min}} = 35$).

Fig. 7. BEAs across different network sizes. Red lines depict the reference scenario costs, aqua-coloured lines the TLD costs for $t_d \in \{t_{d_{\min}}, 30, 91, 183, 274, 365\}$ days. To show when TLD costs amortise, the BEPs are marked by dotted vertical lines — thick ones for $t_{\text{BEP}_{\text{none}}}$, thin ones for $t_{\text{BEP}_{\text{inf}}}$.

The considerable expenses caused by leaks in practice (Section 4.1) highlight the critical importance of implementing LD in general. At the same time, the empirical study shows that this aspect is attributed with a varying degree of urgency and importance, especially where less critical leaks are concerned (Section 3.3). Similarly to other publications [35,48], this study's findings urge for the general adoption of regular LD in DHS monitoring. Beyond that, leaks should be viewed as part of the system's lifecycle, meaning that LD should already be considered during network design.

Modelling leak growth and ongoing cost as part of this study has exposed the critical impact of leaks on economic efficiency. This aspect is key in the fast amortisation of TLD in the BEA, yet – as discussed in Section 4.1.1 – a considerable lack of provided data in this regard makes apparent the current focus on repair. Operators should incorporate ongoing cost calculations into their system assessment when selecting LD methods.

The BEA clearly highlights the economic advantage that aerial TLD can offer for DHS efficiency, but the decision of its usage depends on each network's unique characteristics. The following factors require consideration:

- Defining L_{DHS}: While TLD is pipeline-agnostic (2.3), the applicable area is limited by some factors. This includes installation depth (s. Appendix B) and pipe surroundings, such as barriers that obstruct the line of sight between sensor and ground (train tracks, excessive foliage, etc.). Such areas fall outside the scope of remote sensing-based TIR acquisition and cannot be inspected.
- Defining n_{leaks}: Although the number of leaks has been found to scale with L_{DHS} (Section 3.2), this may not apply to all DHSs. The individual leak rate, assignment to one of the four network categories, and – by extension – applicability of the derived BEA must therefore be checked.
- Defining C_{service}: As shown in Section 4.3, the derived cost for TLD as a UAS service can vary f.e. depending on DHS location. Requesting specific estimates from companies for the given network will provide precise values for individual cost estimations.
- Alternate LD: If other techniques are being implemented, comparisons should be drawn between their costs and application areas (Section 2.2). Given the unique circumstances of each DHS, another method might outweigh TLD in terms of economics or applicability.

Taking these as well as previous chapters into account, DHS operators can assess the economic viability of TLD given their unique circumstances. Marginal cases may also occur, where other forms of implementations are more cost-effective. For S networks with few leaks, hand-held thermographic sensors might be an alternative. Larger networks may consider acquiring the ownership and know-how to carry out UAS flights independently. For XL DHSs, the use of aeroplanes might be more economically viable than UAS [*IX*].

While Section 4.4 highlighted the economic viability of TLD for leak detection, especially given a degree of automation (s. Appendix H, the method also provides other benefits. In the long run, TLD has the potential to be used for large-scale leak monitoring through temporal analyses [14]. While a single TIR acquisition provides only a snapshot of the DHS, data collected across regular UAS flights can be compared to help operators assess their DHS's general condition. This knowledge can form the foundation for more advanced predictive maintenance approaches to schedule repairs before leaks occur [5]. However, as with all methods discussed in Section 2.2, TLD is subject to limitations and may not be capable of assessing a DHS in its entirety. A truly comprehensive LD monitoring strategy should rely on the combination of different techniques to ensure full coverage [7,20].

6. Conclusion and outlook

This study addressed a critical research gap by providing the first quantitative economic evaluation of TLD for leak detection in DHS pipelines, with a specific focus on networks in Central European German-speaking regions. In contrast to other established methods, TLD offers a flexible, scalable, and non-invasive leak localisation approach for all manner of pipe types. Through the integration of new empirical data, a novel form of leak-associated cost was modelled and first-of-its-kind BEA performed. The findings presented in Section 4.4 highlight TLD's potential as a cost-effective tool for leak localisation in networks of all sizes given their short amortisation periods. This study was thereby able to justify the use of TLD for increased system efficiency — not only in terms of cost.

Naturally, it is subject to several limitations. As a case study of Central European German-speaking countries, the observations and findings may not be directly transferable to other regions with different climatic conditions, regulatory frameworks, or DHS infrastructure characteristics. Much of the analysis was developed based on an empirical study consisting of a relatively small number of DHS operators, and the occasionally sparse information required generalisations that may not be representative of all networks.

In order to perform the economic analysis, assumptions needed to be made to model the exemplary leak. In practice, leak growth and repair is defined by a myriad of influencing factors, meaning the cost of a specific leak may differ considerably from the simulated example. The same can be said for DHSs, where each has its own defining characteristics that may differ from the defined four-tier categorisation.

While this study has provided an important initial economic assessment of TLD for DHS leak localisation, there is much potential for future research. To better replicate real-world conditions, exemplary leak modelling can be expanded to simulate different kinds of leak growth in various pipe types. The BEA can be further developed by adjusting for currently disregarded time-dependant changes in cost, such as season-based fluctuations and interim leak repairs. Additional analyses can help assess disregarded financial aspects, such as maintenance intervals and discount rates. Drawing economic comparisons with other LD methods, such as ILDS, could provide additional weight to the results. In this regard, expanding the questionnaire focus and empirical study – for instance to additional European countries or other international regions – would help provide a more solid and more holistic data foundation and enable cross-regional comparisons of leak occurrence, operational practices, and the economic viability of TLD. This would allow for distribution-based instead of fixed-value economic inputs, such as the make-up water cost. On a broader scale, the economic assessment of approaches such as TLD not just for leak detection but also condition monitoring could help shape the future of DHS monitoring.

CRediT authorship contribution statement

Elena Vollmer: Conceptualization, Data curation, Formal analysis, Investigation, Methodology, Validation, Visualization, Writing – original draft, Writing – review & editing. **Rebekka Volk:** Funding acquisition, Writing – review & editing, Supervision. **Frank Schultmann:** Writing – review & editing, Supervision.

Declaration of Generative AI and AI-assisted technologies in the writing process

During the preparation of this work, the authors used ChatGPT (OpenAI) to support technical clarification and expression, as well as explore options for data visualisation and interpretation. After using this tool, the authors reviewed and edited the content as needed and assume full responsibility for the content of the published article.

Declaration of competing interest

The authors declare that they have no known competing financial interests or personal relationships that could have appeared to influence the work reported in this paper.

Acknowledgements

The authors gratefully acknowledge all study participants for their substantive contributions, as well as Marinus Vogl from Air Bavarian GmbH for his valuable assistance in connecting us with district heating operators. This work is supported by funding from the European Union through the AI4EOSC project (Horizon Europe) under Grant number 101058593.

Appendix A. Pipeline installation types and methods

The technical improvement of DHSs throughout the decades is marked by the development of materials that allowed for cost-effective construction. This is particularly true for the pipelines themselves, which constitute the lion's share of network installation costs [45]. Table A.9 presents the different types of pipelines used in DHSs, classified by installation method. While early generation pipes were placed within concrete ducts, the advent of ground-installed PIPs helped overcome the cost barrier and enabled the transition to the third generation [38]. Initial implementations with various casing materials, including fibre or asbestos cement, gave way to plastic, specifically polyurethane rigid foam (PUR) as an insulation material and high-density polyethylene (HDPE) for casings. Combined with steel carriers, composite PIRPs have become the most widely installed pipeline systems today [28].

Appendix B. Acquisition conditions and workflow for TLD

The acquisition-dependent conditions required for collecting high quality TIR images can be summarised as follows:

- Weather-related disturbances can impact the temperature signature on the earth's surface, causing low quality or erroneous TIRs. These disturbances include solar radiation, cloud cover, wind, rain, snowfall, and fog [6,15,48]. Direct sunlight can already cause significant errors in TIR sensor measurements in the far infrared spectrum [51], persistent rain and wind cool down the surface [48], and water droplets in various forms of precipitation greatly reduce resulting image quality [15]. Acquisition should therefore be carried out in dry weather and at low wind speeds [6].

Table A.9
Installation methods and pipeline types (based on Winkens [53], Heating [28], Heipke and Tödter [48], Woods [38] and Roscher [54]).

Installation		Gen	Visualisation	Advantages	Disadvantages	Usage	Carrier & insulation	Casing	Surroundings
Above ground		2, 3	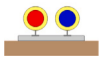	- economical installation, control and repair	- design requirements - exposure to weather and vandalism	Early pipeline type. Mainly implemented for industrial and commercial sites.	Steel / copper with thermal insulation	Metal / plastic	Concrete / steel supports or suspensions
Underground duct-based		1, 2	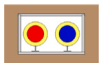	- robust - long life time	- expensive installation and repair - large construction areas	Earliest pipeline type. Nowadays only installed when ductless is not possible or for combined solutions with other pipes.	Metals with thermal insulation	Metal	Concrete or brick
Underground ductless	Pour-in-place	2	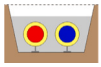	- low installation cost compared to ducts - robust when no installation errors	- more expensive installation than PIP	Intermediary pipeline type. Nowadays outdated in favour of PIP.	Steel	-	- powders with water-resistant additives - bituminous / cement-bonded block insulation
	PIP Glide	3	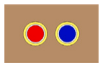	- very high temperature and pressure resistance - lower heat losses due to vacuum	- more expensive than rigid systems	Special application for higher stress conditions (i.e. river culverts, groundwater areas)	Steel with vacuum and mineral fibre	Steel	Ground
	Rigid	3	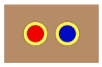	- high temperature and pressure resistance - low installation cost and time	- resistance not as high as for glide systems	Nowadays most prevalent pipeline type.	Steel with PUR *Dated: ductile cast iron*	Plastic (HDPE) *Dated: fibre/ asbestos cement*	Ground
	Flexible	3		- self-compensating - ideal for smaller pipe diameters	- plastic version has limited temperature and pressure resistance	Nowadays most prevalent type for smaller pipe diameters	Cross-linked polyethylene / polybutene or steel / copper with PUR	Plastic (HDPE)	Ground
	Twin	3	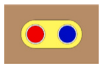	- lower installation cost (smaller trench width) - lower heat loss	- precise routing required, complex routing is costly - only for smaller pipe diameters	Special applications (i.e. house to house connections). Alternative implementation to all PIP single-tube variants.	Steel / PEX / PB with PUR	Plastic (HDPE)	Ground

(a) UAS vehicle for TIR acquisition (b) Raw TIR image (c) Processed TIR with leak

Fig. B.8. TLD exemplified: From TIR image acquisition by UAS to automatic leak detection via analysis software.

- The camera should have an unobstructed view of the ground to ensure no leaks are missed. This includes no insulating layers of foliage or snow [6,15].
- Acquisition should only take place at nighttime or in the early morning when thermal reflectance is lowest, the delta of surrounding temperatures to the network highest, and the TIR sensor most accurate[12] [15,48].
- The carrier temperature in the flow pipe should correspond to the maximum permissible continuous operating temperature and should be constant over a longer period of time so that the heat loss is as constant as possible [48].
- The flow pipe installation depth should be near constant and not exceed 1 m [48].

The practical context of these acquisition conditions is illustrated in Fig. B.8, which shows an example of the UAS-based TIR acquisition workflow, resulting raw imagery, and outputs from automatic image analysis. Further details on the underlying case study and algorithms are discussed in Vollmer et al. [9,15,19].

[12] Pech et al. [52] compare different flight times – 7 AM, 2 PM and 9 PM – and find that midday flights cause considerable variation to ground measurements.

Appendix C. Questionnaire

This appendix lists the set of questions posed to the DHS operators who participated in the study. The first group consists of general questions:

- What is the size of your network (pipe length in km)?
- What types of pipes are installed (percentage of the total network or length in km)?
- How many kilometers of your district heating network are equipped with sensors for leak detection? What specific sensor technology is installed? How reliable is it?
- Do you know of any correlations between leaks and the pipeline age, pipeline type, etc.?
- Have you already had a particularly damaging leak in the network? If so: When was this? What pipeline type did it affect? How high were the losses and repair costs?

A second group of questions revolved around information for a time period (such as per year or higher granularity if available):

- What is the heat production for your network (GWh)?
- What losses are registered (MWh)? What costs are incurred (€/MWh or €/m^3)?

- If there is a general energy loss without leaks, what proportion of the loss is due to leaks?
- How many leaks does your network have per year? How large are they?
- How long does it take to find and repair leaks? What costs are incurred with the methods currently used to locate leaks in pipes?
- What costs are incurred in the event of a falsely located leak, i.e. by excavating at the incorrect place?

Appendix D. Sensitivity analysis of leak cost modelling for cumulative cost

A SA is performed to assess how the parameters defining ongoing and one-time repair costs influence the cumulative leak cost. The relevant parameters are given in Eqs. (2) and (4).

For the ongoing cost assessment, the modelled leak growth as defined in Eq. (3) is complemented by lower- and upper-bound scenarios. While the baseline was intentionally defined as a conservative but practically relevant leak progression, lower- and upper-bound cases are considered to test the robustness of the conclusions to uncertainty in this type of leak development. Given the mathematical interdependence of growth functions parameters, simply varying individual values can result in physically unrealistic curves. Therefore, plausible parameter combinations are defined instead of iterating through all mathematically possible values.

For the Richards-based leak growth model, the maximum leak flow rate a and growth coefficient c are varied, while the inflection point b and curve steepness N are kept constant. This preserves the assumed pipe-diameter context and general leak class while allowing the analysis of differences in leak magnitude and progression speed. A lower-bound scenario ($a = 25\,m^3/day$, $c = 0.009$) and upper-bound ($a = 35\,m^3/day$, $c = 0.011$) are defined, resulting in the curves depicted in Fig. D.9. These selections ensure a valid test of uncertainty while staying within or below the conservative range defined in literature and the empirical study. The lower bound remains below $10\,m^3/day$ at 6 months and $20\,m^3/day$ at a year, while the upper case barely exceeds $15\,m^3/day$ and $30\,m^3/day$ respectively.

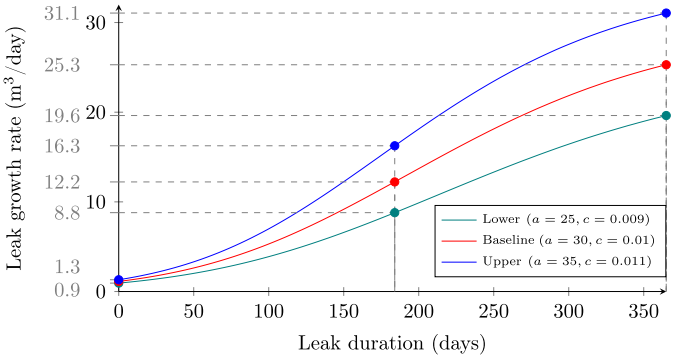

Fig. D.9. Scenarios for exemplary leak growth using lower-, baseline- (a =30 m^3/day, $b = 1$, $c = 0.01$, $N = 0.4$), and upper-bound Richards curves.

The final parameter influencing ongoing cost is $C_{make-up}$. Since the most conservative reported value was already selected for the baseline scenario, only an additional upper bound of $7 €/m^3$ is defined for the SA. This ensures that all empirical values lie within the defined range and provides a suitable basis for assessing uncertainty in the make-up water cost assumption.

For repair costs, lower- and upper-bound scenarios are defined from empirically motivated values to reflect varying degrees of situational complexity (see Fig. D.10). In the lower-bound scenario (a = 15,000 €, $b = 1.75$, $c = 0.01$), the parameters are matched to the minimum reported repair cost of 2000 € and the lower-end average for long-term repairs of 13,000 €. For the upper-bound (a = 25,000 €, b = 1.45, $c = 0.014$), the curve reflects faster cost escalation associated with more complex urban infrastructure, starting at the higher end of reported minimum cost for repairs (5000 €) and reaching nearly 25,000 € after one year. By varying the growth coefficient c, the analysis accounts for uncertainty not just in the total cost magnitude, but also in the speed at which situational complications arise.

With these parameter choices, a lower-bound scenario cost-minimising and upper bound cost-increasing case are defined. While the baseline scenario used in this study is the most likely representation of the exemplary leak, these can be interpreted as a boundary corridor for the same conservative leak class.

Table D.10 shows how the described parameter variations affect the cumulative leak cost. As the cost differences after one year (C_{total} (t = 365)) indicate, the assumed parameter combinations have a substantial influence on the magnitude of the result. However, the qualitative finding from the baseline remains unchanged across all scenarios: Ongoing costs account for more than half of total leak cost after one year.

Relative to the baseline, the lower- and upper-bound growth and repair scenarios change the one-year total leak cost by around -28 % and +29 %, respectively. Increasing $C_{make\text{-}up}$ from 5 to $7 €/m^3$ increases the one-year total cost by ca. 22 % and shifts the parity point t_p – the day at which cumulative ongoing costs exceed repair costs — forward by 55 to 61 days. In comparison, varying the growth and repair scenarios with a fixed make-up water cost changes t_p by 21 to 27 days. For the conservative leak type considered here, $C_{make\text{-}up}$ therefore has the strongest influence on the point in time when ongoing costs start to dominate C_{total}.

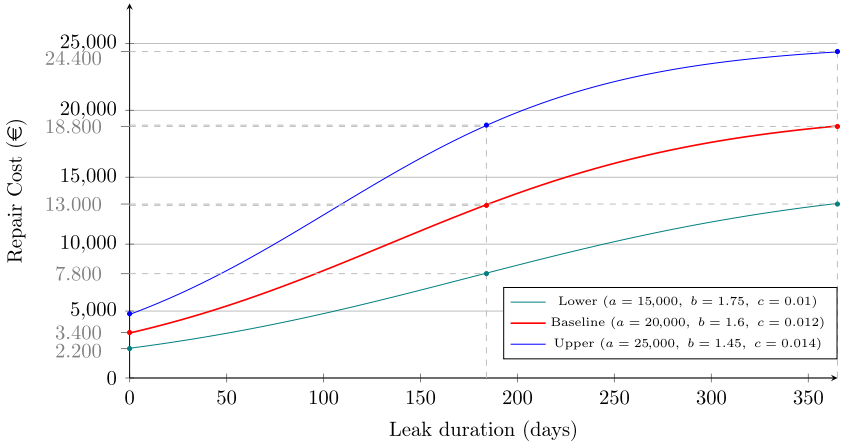

Fig. D.10. Scenarios for exemplary repair cost growth using lower-, baseline- (a =20,000 €, $b = 1.6$, $c = 0.012$), and upper-bound sigmoid curves.

Table D.10
Impact of parameter variations in lower-, baseline, and upper-bound cost scenarios on cumulative cost and cost parity between ongoing and repair components.

Growth model	$C_{\text{make-up}}$ [€ / m^3]	$C_{\text{total}}(t = 365)$ [€]	$C_{\text{ongoing}}(t = 180)$ share [%]	$C_{\text{ongoing}}(t = 365)$ share [%]	t_p [days]
Lower-bound		30,037.18	31.88	56.56	310
Baseline	5	41,653.06	27.87	54.79	328
Upper-bound		53,617.53	25.84	54.54	331
Lower-bound		36,832.71	39.59	64.57	249
Baseline	7	50,781.59	35.11	62.92	270
Upper-bound		65,315.41	32.78	62.68	276

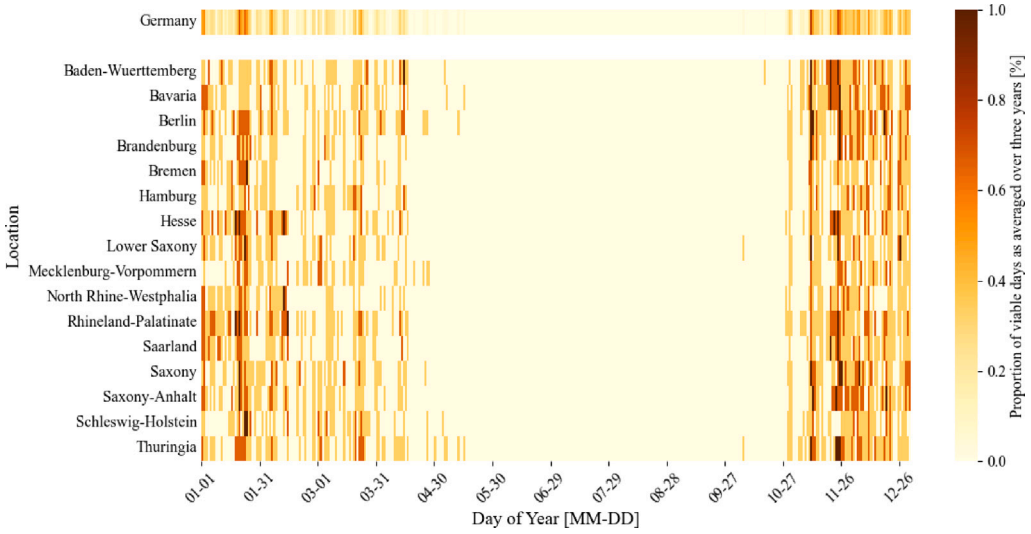

Fig. E.11. Viable days for TIR image acquisition across Germany and its various states (based on weather data from Meteostat [55]).

Appendix E. Estimating the viable day count for TLD

Historical weather data from Meteostat [55] are analysed to estimate the number of days that high-quality TIR images can be acquired. To this end, weather stations located within the largest city in each German state are selected to represent the different regions. For a representative assessment, an investigation period of three consecutive years is selected, specifically 2019, 2020, and 2021.[13] Daily measurements are used to identify when the stringent conditions as per Appendix B were met. Specifically, these are defined as:

1. a maximum temperature below 10 °C ($T_{\max} < 10$ °C),
2. a minimum temperature below 5 °C ($T_{\min} < 5$ °C),
3. no precipitation ($prcp = 0$ mm),
4. no snowfall ($snow = 0$ mm),
5. an average wind speed below 5 m/s ($wspd < 5$ m/s).

Fig. E.11 displays the results of the analysis averaged for each of the different states as well as across Germany. Acceptable time frames generally range from fall to spring, whereby periods of consistently favourable conditions are found in November, mid-January, and mid-March. This indicates that multiple acquisitions could be organised for DHS assessment, such as at the beginning and end of the main operating season.

In terms of quantification, Fig. E.12 visualises the number of viable days per year for data acquisition throughout Germany. While the box plots highlight to what extent this value may differ depending on the year in question, the median is found to lie within a comparatively similar range of between 35 and 43 days. The combination of these values, shown in the overall box plot, depicts a median of around 39, which is almost identical to the overall average of 40 days. This latter value will therefore be used as an underlying assumption for the economic viability analysis.

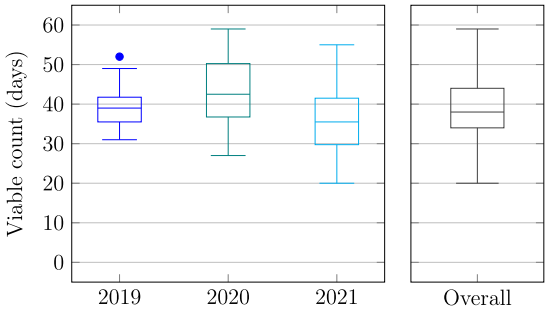

Fig. E.12. Box plots of viable day counts for TIR image acquisition per year across all German states (based on weather data from Meteostat [55]).

Appendix F. Breakdown of the BEA

Table F.11 gives a quantitative overview of the BEA results, detailing the values that are visualised in Fig. 7. Similarly to there, TC_{none} (Eq. (9)) and TC_{inf} (Eq. (8)) are compared to TC_{TLD} (Eq. (10)). t_{BEP} is the number of days at which the BEP is reached for both of those comparisons, while Δt_{BEP} is the number of days after which the BEP is

[13] These specific years were chosen as they were the only ones in the past decade for which data was consistently available for all days [55].

Table F.11
Breakdown of BEA results for all networks sizes.

t_d scenario	Parameter	Unit	S		M		L		XL	
			TC_{none}	TC_{inf}	TC_{none}	TC_{inf}	TC_{none}	TC_{inf}	TC_{none}	TC_{inf}
$t_{d_{min}}$	t_{BEP}	days	100	243	76	220	80	224	87	230
	Δt_{BEP}	days	92	235	66	210	63	207	52	195
	TC_{TLD}	€	9422.97		37 753.95		140 974.56		459 298.95	
30	t_{BEP}	days	112	254	89	232	88	232	–	–
	Δt_{BEP}	days	82	224	59	202	58	202	–	–
	TC_{TLD}	€	10 451.05		42 467.75		152 343.9		–	
91	t_{BEP}	days	153	294	134	276	133	275	129	272
	Δt_{BEP}	days	62	203	43	185	42	184	38	181
	TC_{TLD}	€	14 446.79		62 446.45		224 267.22		664 635.95	
183	t_{BEP}	days	231	372	215	356	215	356	212	353
	Δt_{BEP}	days	48	189	32	173	32	173	29	170
	TC_{TLD}	€	23 615.91		108 292.05		389 311.38		1 168 937.55	
274	t_{BEP}	days	317	456	303	442	303	442	300	439
	Δt_{BEP}	days	43	182	29	168	29	168	26	165
	TC_{TLD}	€	34 999.9		165 212		594 223.2		1 795 057	
365	t_{BEP}	days	406	543	392	529	392	529	390	527
	Δt_{BEP}	days	41	178	27	164	27	164	25	162
	TC_{TLD}	€	47 390.56		227 165.3		817 255.08		2 476 543.3	

Table G.12
Impact of smallest, baseline, and highest leak cost scenarios on BEA results for S and XL networks and reference scenario TC_{none}.

Growth model	$C_{\text{make-up}}$ [€/m³]	Parameter for TC_{none}	S		XL	
			$t_d = t_{d_{min}}$	$t_d = 365$	$t_d = t_{d_{min}}$	$t_d = 365$
Lower-bound	5	t_{BEP}	139	415	113	395
		Δt_{BEP}	131	50	78	30
Baseline	5	t_{BEP}	100	406	87	390
		Δt_{BEP}	92	41	52	25
Upper-bound	7	t_{BEP}	71	391	69	380
		Δt_{BEP}	63	26	34	15

reached after localisation and repair ($\Delta t_{\text{BEP}} = t_{\text{BEP}} - t_d$). The total cost at BEP is the same for both comparisons, as it is equal to $TC_{\text{TLD}}(t_d)$.

Appendix G. Sensitivity analysis of leak cost modelling for BEA

To assess the robustness of the BEA with respect to leak cost modelling, the lower-, baseline, and upper-bound cumulative cost scenarios defined in Appendix D are applied to select BEA cases. Table G.12 summarises the resulting break-even day t_{BEP} and amortisation period Δt_{BEP} for representative S and XL networks with both minimum ($t_d = t_{d_{min}}$) and late ($t_d = 365$) leak removal, using reference scenario TC_{none}. To capture the widest plausible sensitivity range, the baseline is compared to the smallest (lower-bound with $C_{\text{make-up}} = 5$ €/m³) and highest (upper-bound with $C_{\text{make-up}} = 7$ €/m³) leak cost scenarios.

While the exact break-even timing shifts across scenarios, the qualitative outcome of the BEA remains unchanged. TLD amortises within a comparatively short period after leak removal in all tested cases, ranging from 15 to 131 days. This indicates that the economic viability of TLD is robust to plausible lower- and upper-bound variations in leak growth, make-up water cost, and repair cost modelling. As in the baseline analysis, larger networks and longer leak removal times continue to result in faster amortisation.

Relative to the baseline, the smallest leak cost scenario increases the amortisation period by approximately 20 % to 50 %, while the highest reduces it by around 32 % to 40 %. Interestingly, the smallest scenario has a larger relative impact on Δt_{BEP}. This is due to the non-linear nature of the modelling: slower leak growth and repair cost escalation reduce the rate at which the reference scenario TC_{none} accumulates costs. Consequently, the avoided cost grows more slowly, delaying the amortisation of the fixed C_{TLD} more significantly than higher leak costs accelerate it. This asymmetry implies that the amortisation period of TLD is more sensitive to underestimating leak costs than to comparably pessimistic overestimations. However, since even the smallest cost scenario still amortises within roughly four months, the fundamental decision to implement TLD remains robust in the explored range of C_{ongoing} and C_{repair} uncertainties.

Appendix H. Sensitivity analysis of TLD automation for BEA

This appendix provides details on the impact that automating the analysis step has on TLD cost given the associated reduction of C_{analysis}. Fig. H.13 shows how this choice influences each BEA for the various network sizes as visual SAs. As in Fig. 7, the aqua-toned lines show the TC_{TLD} costs depending on t_d (Eq. (10), with $C_{\text{service}} = 337.5$ €/km given a 25 % savings through C_{analysis} automation (Eq. (7)). As described in Section 4.3, this was the most conservative choice given the possible range of 25 % to 40 % that manual C_{analysis} currently contributes to the total cost. To assess the impact of said choice, this value range is depicted visually as the coloured, filled in areas below each aqua-toned line, where the 40 % maximum savings scenario are at the lower edge of each area. The dotted lines above the 25%-savings scenario represent the current status quo – no automation of C_{analysis} – as a baseline.

The comparison is based solely on monetary savings, without taking into account the time delay to which the baseline scenario is inherently subject, given that manual image viewing may require up multiple weeks depending on the network size.[14] Despite this, Fig. H.13 shows a significant difference between baseline and the savings scenarios. Even the most conservatively assumed automation enables TLD costs to amortise faster for $t_d = 1$ month than they do for the $t_{d_{\text{min}}}$ baseline.

Given the linearity of C_{TLD} and its sole dependency on L_{DHS}, the absolute cost difference to the baseline is constant for a network, regardless of t_d. This means that in terms of percentage, savings are more impactful earlier on. In the S network, for instance, cost savings for $t_{d_{\text{min}}}$ amount to 17 % in the minimum savings scenario (25 %) and can reach up to 27 % for the maximum scenario (40 %). Given the much higher cost at $t_d = 365$ days, the savings here comprise only 4 % and 6 % of the total, respectively. However, amortisation is a different matter. As indicated above, the relevance of automation and associated

[14] According to [15], around 1300 images are acquired per km pipeline, which assuming a fast viewing speed of 1 s/imagealready results in 25 days for XL networks.

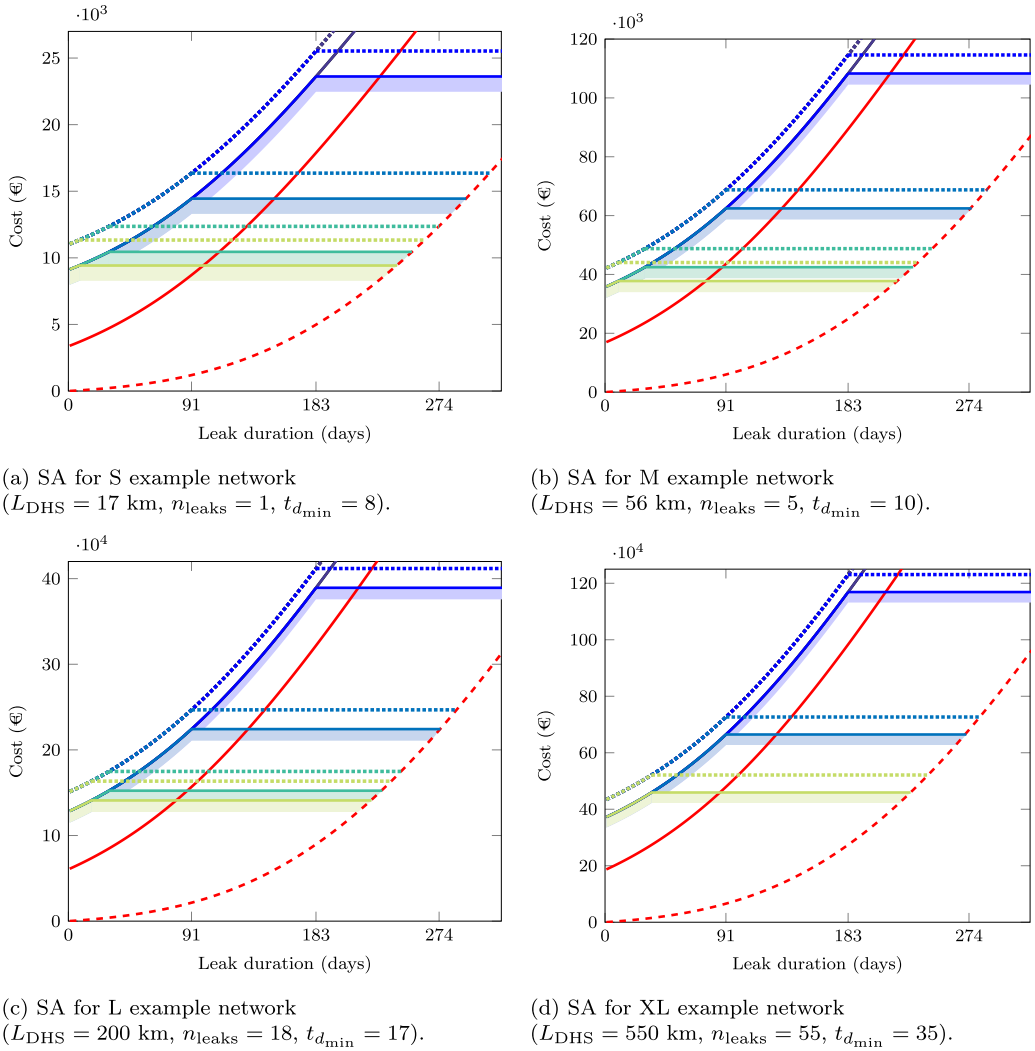

(a) SA for S example network ($L_{\text{DHS}} = 17$ km, $n_{\text{leaks}} = 1$, $t_{d_{\min}} = 8$).

(b) SA for M example network ($L_{\text{DHS}} = 56$ km, $n_{\text{leaks}} = 5$, $t_{d_{\min}} = 10$).

(c) SA for L example network ($L_{\text{DHS}} = 200$ km, $n_{\text{leaks}} = 18$, $t_{d_{\min}} = 17$).

(d) SA for XL example network ($L_{\text{DHS}} = 550$ km, $n_{\text{leaks}} = 55$, $t_{d_{\min}} = 35$).

Fig. H.13. SAs for the impact of automation on TLD cost across different network sizes.

savings plays a key role. Compared to TC_{none}, the most conservative automation reduces the time Δt_{BEP} by at least 19.3 % ($t_{d_{\min}}$) and up to 25.45 % ($t_d = 365$ days) for S networks. These numbers increase with network size, amounting to 21.2 % to 26.5 % for XL networks.

A comparison between the different savings scenarios shows that increased automation is greatly beneficial and increases in relevance as time passes. For S networks, for instance, an additional 15 % automation achieves 12.3 % faster amortisation for Δt_{BEP} compared, which increases to 14.6 % at $t_d = 365$ days. These values also grow with network size, reaching 13.6 % to 14.7 % for XL networks — and therefore a 34.9 % to 41.2 % reduction through maximum automation. This means that, given time, automating C_{analysis} by a given percentage results in an even greater percentage reduction in the amortisation time Δt_{BEP}.

Data availability

The data that has been used is confidential.

References

[1] Euroheat & Power, DHC Market Outlook 2024, Technical Report, Euroheat & Power, Brussels, Belgium, 2024, URL https://www.euroheat.org/data-insights/outlooks/dhc-market-outlook-2024.

[2] International Energy Agency (IEA), Technology and Innovation Pathways for Zero-carbon-ready Buildings by 2030, Technical Report, IEA, 2022, URL https://www.iea.org/reports/technology-and-innovation-pathways-for-zero-carbon-ready-buildings-by-2030.

[3] Arbeitsgemeinschaft Fernwärme [Consortium on District Heating] (AGFW), Hauptbericht 2022 [Main report 2022], Technical Report, AFGW Energieeffizienzverband für Wärme, Kälte und KWK e.V., Frankfurt am Main, 2023.

[4] Xiaofang Shan, Peng Wang, Weizhen Lu, The reliability and availability evaluation of repairable district heating networks under changeable external conditions, Appl. Energy 203 (2017) 686–695, http://dx.doi.org/10.1016/j.apenergy.2017.06.081.

[5] Amir Rafati, Hamid Reza Shaker, Predictive maintenance of district heating networks: A comprehensive review of methods and challenges, Therm. Sci. Eng. Prog. 53 (2024) 102722, http://dx.doi.org/10.1016/j.tsep.2024.102722.

[6] Ola Friman, Peter Follo, Jorgen Ahlberg, Stefan Sjokvist, Methods for large-scale monitoring of district heating systems using airborne thermography, IEEE Trans. Geosci. Remote Sens. 52 (8) (2014) 5175–5182, http://dx.doi.org/10.1109/TGRS.2013.2287238.

[7] Samer El-Zahab, Tarek Zayed, Leak detection in water distribution networks: an introductory overview, Smart Water 4 (1) (2019) 5, http://dx.doi.org/10.1186/s40713-019-0017-x.

[8] International Energy Agency (IEA), World Energy Investment 2020, Technical Report, IEA, Paris, 2020, URL https://www.iea.org/reports/world-energy-investment-2020. Licence: CC BY 4.0.

[9] Elena Vollmer, Julian Ruck, Rebekka Volk, Frank Schultmann, Detecting district heating leaks in thermal imagery: Comparison of anomaly detection methods, Autom. Constr. 168 (2024) 105709, http://dx.doi.org/10.1016/j.autcon.2024.105709.

[10] Shoujun Zhou, Zheng O'Neill, Charles O'Neill, A review of leakage detection methods for district heating networks, Appl. Therm. Eng. 137 (2018) 567–574, http://dx.doi.org/10.1016/j.applthermaleng.2018.04.010.

[11] Jawwad Latif, Muhammad Zeeshan Shakir, Neil Edwards, Marcin Jaszczykowski, Naeem Ramzan, Victoria Edwards, Review on condition monitoring techniques for water pipelines, Measurement 193 (2022) 110895, http://dx.doi.org/10.1016/j.measurement.2022.110895.

[12] S.-A. Ljungberg, M. Rosengren, Aerial thermography - A tool for detecting heat losses and defective insulation in building attics and district heating networks, in: Thermosense IX: Thermal Infrared Sensing for Diagnostics and Control, Vol. 0780, International Society for Optics and Photonics, SPIE, Orlando, United States, 1987, pp. 257–343, http://dx.doi.org/10.1117/12.940525.

[13] S. Axelsson, Thermal modeling for the estimation of energy losses from municipal heating networks using infrared thermography, IEEE Trans. Geosci. Remote Sens. 26 (5) (1988) 686–692, http://dx.doi.org/10.1109/36.7695.

[14] Amanda Berg, Jörgen Ahlberg, Michael Felsberg, Enhanced analysis of thermographic images for monitoring of district heat pipe networks, Pattern Recognit. Lett. 83 (2016) 215–223, http://dx.doi.org/10.1016/j.patrec.2016.07.002.

[15] Elena Vollmer, Rebekka Volk, Frank Schultmann, Automatic analysis of UAS-based thermal images to detect leakages in district heating systems, Int. J. Remote Sens. (2023) http://dx.doi.org/10.1080/01431161.2023.2242586.

[16] Yanfei Zhong, Yao Xu, Xinyu Wang, Tianyi Jia, Guisong Xia, Ailong Ma, Liangpei Zhang, Pipeline leakage detection for district heating systems using multisource data in mid- and high-latitude regions, ISPRS J. Photogramm. Remote Sens. 151 (2019) 207–222, http://dx.doi.org/10.1016/j.isprsjprs.2019.02.021.

[17] A. Sledz, C. Heipke, Thermal anomaly detection based on saliency analysis from multimodal imaging sources, ISPRS Ann. Photogramm. Remote. Sens. Spat. Inf. Sci. V-1-2021 (2021) 55–64, http://dx.doi.org/10.5194/isprs-annals-V-1-2021-55-2021.

[18] Kabir Hossain, Frederik Villebro, Søren Forchhammer, UAV image analysis for leakage detection in district heating systems using machine learning, Pattern Recognit. Lett. 140 (2020) 158–164, http://dx.doi.org/10.1016/j.patrec.2020.05.024.

[19] Elena Vollmer, Julian Ruck, Rebekka Volk, Frank Schultmann, Leak detection using thermal imagery: Deep learning versus traditional computer vision state-of-the-art, ISPRS J. Photogramm. Remote Sens. 228 (2025) 505–518, http://dx.doi.org/10.1016/j.isprsjprs.2025.06.006.

[20] Lijun Tuikka, Leak Detection Systems in Finnish District Heating Network (Bachelor thesis), Tampere University of Applied Sciences, Finland, 2024.

[21] Shengtao Ye, Fuzhong Yu, Min Hao, Menghai Wu, Dandan Chen, Changsheng Bu, Ping Lu, Yuntan Du, Kaige Cui, Leakage diagnosis technologies for heating pipe networks: A comprehensive review of currently used methods, Int. J. Energy Res. 2025 (1) (2025) 8824853, http://dx.doi.org/10.1155/er/8824853.

[22] S.M. Masum Ahmed, Annamaria Bagaini, Edoardo Croci, District heating benefits and economic assessment methods: A systematic review and the role of emerging technologies, Energies 18 (24) (2025) 6464, http://dx.doi.org/10.3390/en18246464.

[23] Cristina Sáez Blázquez, Arturo Farfán Martín, Ignacio Nieto, Diego González-Aguilera, Economic and environmental analysis of different district heating systems aided by geothermal energy, Energies 11 (5) (2018) 1265, http://dx.doi.org/10.3390/en11051265.

[24] Hrvoje Dorotić, Kristijan Čuljak, Josip Miškić, Tomislav Pukšec, Neven Duić, Technical and economic assessment of supermarket and power substation waste heat integration into existing district heating systems, Energies 15 (5) (2022) 1666, http://dx.doi.org/10.3390/en15051666, URL https://www.mdpi.com/1996-1073/15/5/1666.

[25] Roman Geyer, Jürgen Krail, Benedikt Leitner, Ralf-Roman Schmidt, Paolo Leoni, Energy-economic assessment of reduced district heating system temperatures, Smart Energy 2 (2021) 100011, http://dx.doi.org/10.1016/j.segy.2021.100011.

[26] Henrik Lund, Sven Werner, Robin Wiltshire, Svend Svendsen, Jan Eric Thorsen, Frede Hvelplund, Brian Vad Mathiesen, 4Th generation district heating (4GDH): Integrating smart thermal grids into future sustainable energy systems, Energy 68 (2014) 1–11, http://dx.doi.org/10.1016/j.energy.2014.02.089.

[27] Sven Werner, International review of district heating and cooling, Energy 137 (2017) 617–631, http://dx.doi.org/10.1016/j.energy.2017.04.045.

[28] Q.M. District Heating, Handbook on Planning of District Heating Networks, version 1.0 ed., Swiss Federal Office of Energy (SFOE), Bern, Switzerland, ISBN: 3-908705-39-8, 2020.

[29] Ding Mao, Peng Wang, Yi-Ping Fang, Long Ni, Understanding district heating networks vulnerability: A comprehensive analytical approach with controllability consideration, Sustain. Cities Soc. 101 (2024) 105068, http://dx.doi.org/10.1016/j.scs.2023.105068.

[30] I Žutautaite, J Augutis, R Krikštolaitis, G Dundulis, M Valinčius, S Rimkevičius, Risk and reliability assessment of the district heating network methodology with case study, in: Lesley Walls, Matthew Revie, Tim Bedford (Eds.), Risk, Reliability and Safety: Innovating Theory and Practice, CRC Press, Taylor & Francis Group, 6000 Broken Sound Parkway NW, Suite 300, Boca Raton, FL 33487-2742, ISBN: 978-1-138-02997-2, 2016, pp. 2578–2585, http://dx.doi.org/10.1201/9781315374987-391.

[31] Enzo Losi, Lucrezia Manservigi, Pier Ruggero Spina, Mauro Venturini, Data-driven approach for the detection of faults in district heating networks, Sustain. Energy Grids Netw. 38 (2024) 101355, http://dx.doi.org/10.1016/j.segan.2024.101355.

[32] Aleksandr Hlebnikov, Anna Volkova, Olga Dzuba, Arvi Poobus, Ülo Kask, Damages of the tallinn district heating networks and indicative parameters for an estimation of the networks general condition, Sci. J. Riga Tech. Univ. Environ. Clim. Technol. 5 (-1) (2010) http://dx.doi.org/10.2478/v10145-010-0034-3.

[33] Verband Fernwärme Schweiz [Association for District Heating in Switzerland] (VFS), Leitfaden Fernwärme / Fernkälte, Schlussbericht [Final Report] 1.3, Bundesamt für Energie (BFE), Bern, 2022.

[34] I.I. Murtazin, M.V. Kozhevnikov, E.M. Starikov, Development and application of methods of internal inspection of district heating networks, Int. J. Energy Prod. Manag. 6 (1) (2021) 56–70, http://dx.doi.org/10.2495/EQ-V6-N1-56-70.

[35] K. Wojdyga, M. Chorzelski, Chances for polish district heating systems, Energy Procedia 116 (2017) 106–118, http://dx.doi.org/10.1016/j.egypro.2017.05.059.

[36] Ramuné Gurklienė, William Hogland, Håkan Knutsson, Valdas Lukosevičius, Jelena Lundström, Magnus Ohlsson, Andrzej Rogala, Piotr Rybarczyk, Kamil Zajaczkowski, BSAM Data Driven Proactive Maintenance Handbook: Smart Maintenance of District Heating Networks, Linnaeus University, Department of Biology and Environmental Science, Kalmar, ISBN: 978-91-8082-036-3, 2023.

[37] Arbeitsgemeinschaft Fernwärme [Consortium on District Heating] (AGFW), Verfahren zur Zustandsermittlung von Fernwärmeleitungen und zur Feststellung/Einmessung von Abweichungen (Leckortung) [Methods for Assessing the Condition of District Heating Pipelines and for Locating Deviations (Leak Detection)], Fachbericht [Technical Report] FW 435, AGFW, Frankfurt am Main, Germany, 2023.

[38] Paul Woods, An Introduction to District Heating and Cooling: Low Carbon Energy for Buildings, IOP Publishing, ISBN: 978-0-7503-5286-4, 2023, http://dx.doi.org/10.1088/978-0-7503-5286-4.

[39] Panos Konstantin, Margarete Konstantin, Praxisbuch der Fernwärme- und Fernkälteversorgung: Systeme, Netzaufbauvarianten, Kraft-Wärme- und Kraft-Wärme-Kälte-Kopplung, Kostenstrukturen und Preisbildung, third ed., Springer Berlin Heidelberg, Berlin, Heidelberg, ISBN: 978-3-662-69526-5, 2024, http://dx.doi.org/10.1007/978-3-662-69526-5.

[40] Arbeitsgemeinschaft Fernwärme [Consortium on District Heating] (AGFW), Praxishilfe "Fernwärmeleitungsbau – Verlegesysteme und Kosten" [Practical Guide: "District Heating Pipeline Construction – Systems and Costs"], Technical Report, AGFW Der Energieeffizienzverband für Wärme, Kälte und KWK e. V, Frankfurt am Main, 2021, URL https://www.agfw.de/technik-normung/aktuelles-aus-dem-bereich/newsdetail/praxishilfe-fernwaermeleitungsbau-verlegesysteme-und-kosten.

[41] LANCIER Monitoring GmbH, LANCIER monitoring, 2025, URL https://www.lancier-monitoring.de/en/.

[42] Miguel Gonzalez-Salazar, Thomas Langrock, Christoph Koch, Jana Spieß, Alexander Noack, Markus Witt, Michael Ritzau, Armin Michels, Evaluation of energy transition pathways to phase out coal for district heating in Berlin, Energies 13 (23) (2020) 6394, http://dx.doi.org/10.3390/en13236394.

[43] H.V. Fuchs, W. Frommhold, Leckortung auf fernwärmeleitungen, IBP Mitteilungen 18 (201) (1991) URL https://www.ibp.fraunhofer.de/content/dam/ibp/ibp-neu/de/dokumente/ibpmitteilungen/1-400/201-300/201_IBPmitteilung.pdf.

[44] Arbeitsgemeinschaft Fernwärme [Consortium on District Heating] (AGFW), Instandhaltungsstrategien und Rehabilitationsplanung - Mindestanforderungen [Maintenance Strategies and Rehabilitation Planning - Minimum Requirements], Merkblatt [Fact Sheet] FW 114, AGFW, 2013.

[45] Abdur Rehman Mazhar, Shuli Liu, Ashish Shukla, A state of art review on the district heating systems, Renew. Sustain. Energy Rev. 96 (2018) 420–439, http://dx.doi.org/10.1016/j.rser.2018.08.005.

[46] Guancheng Guo, Shuming Liu, Dailin Jia, Shanhe Wang, Xue Wu, Simulation of a leak's growth process in water distribution systems based on growth functions, AQUA Water Infrastruct. Ecosyst. Soc. 70 (4) (2021) 521–536, http://dx.doi.org/10.2166/aqua.2021.021.

[47] John H.M. Thornley, James France, An open-ended logistic-based growth function, Ecol. Model. 184 (2–4) (2005) 257–261.

[48] C. Heipke, J. Tödter, Drohnengestützte Thermografie als Basis der Asset- und Instandhaltungsstrategie von Fern- und Nahwärmenetzen [Drohne-based Thermography as an Asset- and Maintenancestrategy for District Heating Systems], Schlussbericht [Final Report] IGF-Vorhaben Nr. 19768 N, Fernwärme-Forschungsinstitut in Hannover e.V. (FFI) and Leibniz Universität Hannover, Institut für Photogrammetrie und GeoInformation (IPI), 2020.

[49] Axel Clouet, The thermal imaging and sensing market since 2019, in: Nicolas P. Avdelidis (Ed.), Thermosense: Thermal Infrared Applications XLV, SPIE, Orlando, United States, 2023, p. 34, http://dx.doi.org/10.1117/12.2664172, ISBN: 978-1-5106-6186-8 978-1-5106-6187-5.

[50] Paula Höhrová, Jakub Soviar, Włodzimierz Sroka, Market analysis of drones for civil use, LOGI Sci. J. Transp. Logist. 14 (1) (2023) 55–65, http://dx.doi.org/10.2478/logi-2023-0006.

[51] H. Madura, M. Kołodziejczyk, Influence of sun radiation on results of non-contact temperature measurements in far infrared range, Opto-Electron. Rev. 13 (2005) 253–257.

[52] K. Pech, N. Stelling, P. Karrasch, H.-G. Maas, Generation of multitemporal thermal orthophotos from UAV data, Int. Arch. Photogramm. Remote. Sens. Spat. Inf. Sci. XL-1/W2 (2013) 305–310, http://dx.doi.org/10.5194/isprsarchives-XL-1-W2-305-2013.

[53] H.-P. Winkens, Fernwärmespeicherung, -Transport Und Verteilung [District Heating Storage, Transportation and Distribution], Project Report 4, Institut für Energiewirtschaft und Rationelle Energieanwendung (IER) der Universität Stuttgart, Mannheim, 1993.

[54] Harald Roscher, Rehabilitation von fernwärmekanälen und fernwärmeleitungen, in: Hans-Burkhard Horlacher, Ulf Helbig (Eds.), Rohrleitungen 2, Springer Berlin Heidelberg, Berlin, Heidelberg, ISBN: 978-3-662-60803-6, 2023, pp. 1199–1231, http://dx.doi.org/10.1007/978-3-662-60804-3_69.

[55] Meteostat, Meteostat: Free historical weather and climate data, 2024, URL https://meteostat.net. Weather data for Germany sourced via the German Weatherservice (Deutscher Wetterdienst).